The Evaluation of the Numerical Methods to Study the Buckling of Stiff Films on Elastomeric Substrates

by

Swathi Sri Kondagari

A Thesis Presented in Partial Fulfillment
of the Requirements for the Degree
Master of Science

Approved November 2010 by the
Graduate Supervisory Committee:

Hanqing Jiang, Chair
Hongyu Yu
Subramaniam Rajan

ARIZONA STATE UNIVERSITY

December 2010

ABSTRACT

Ordered buckling of stiff films on elastomeric substrates has many applications in the field of stretchable electronics. Mechanics plays a very important role in such systems. A full three dimensional finite element analysis studying the pattern of wrinkles formed on a stiff film bonded to a compliant substrate under the action of a compressive force has been widely studied. For thin films, this wrinkling pattern is usually sinusoidal, and for wide films the pattern depends on loading conditions. The present study establishes a relationship between the effect of the load applied at an angle to the stiff film.

A systematic experimental and analytical study of these systems has been presented in the present study. The study is performed for two different loading conditions, one with the compressive force applied parallel to the film and the other with an angle included between the application of the force and the alignment of the stiff film. A geometric model closely resembling the experimental specimen studied is created and a three dimensional finite element analysis is carried out using ABAQUS (Version 6.7).

The objective of the finite element simulations is to validate the results of the experimental study to be corresponding to the minimum total energy of the system. It also helps to establish a relation between the parameters of the buckling profile and the parameters (elastic and dimensional parameters) of the system. Two methods of non-linear analysis namely, the Newton-Raphson method and Arc-Length method are used. It is found that the Arc-Length method is the most cost effective in terms of total simulation time for large models (higher number of

elements).The convergence of the results is affected by a variety of factors like the dimensional parameters of the substrate, mesh density of the model, length of the substrate and the film, the angle included.

For narrow silicon films the buckling profile is observed to be sinusoidal and perpendicular to the direction of the silicon film. As the angle increases in wider stiff films the buckling profile is seen to transit from being perpendicular to the direction of the film to being perpendicular to the direction of the application of the pre-stress. This study improves and expands the application of the stiff film buckling to an angled loading condition.

ACKNOWLEDGMENTS

I would like to thank Arizona State University for providing me an opportunity to perform this research work. I am deeply indebted to my advisor Dr. Hanqing Jiang for advising me and for the direction he has lent to this project. His expertise and insight have been influential in performing this research work. His teaching and work ethic are an inspiration. I would also like to thank the members of my supervisory committee, Dr. Subramaniam Dharma Rajan and Dr. Hongyu Yu for their support. I thank Dr. Cunjiang Yu for providing us with the experimental data and the constant support. I would like to thank all my lab mates for providing constant support throughout the two years of my thesis. I am also obliged to the faculty of the Mechanical Engineering group at Arizona State University for their guidance, and the students for their companionship. I'd also like to thank the High Performance Computing Center (HPCI) for their help in running the high power finite element simulations. Finally, I'd like to thank the department of Mechanical and Aerospace engineering, the graduate advisors Dr. Lynn Cozort and Dr.Sharon Yee and our department chair Dr. Kyle Squires for their support.

Last but never the least, I would like to thank my parents, Mrs. & Mr. Kondagari for having been there through all my hardships and helping me sail through them in the best possible frame of mind.

TABLE OF CONTENTS

Page

LIST OF TABLES

LIST OF FIGURES

Figure Page

1 INTRODUCTION

A stiff film (metal) on a compliant substrate (an elastomer) under application of a compressive force on the elastomer forms ordered wrinkles on the stiff film was reported first by (N. Bowden, W. T. Huck, et al. 1998). Since then, there has been a lot of interest in flexible/stretchable electronics which are mechanically deformable while maintaining their functionalities. Other than using organic materials of natural flexibility or stretchability to realize their device configurations, very recently, flexible and stretchable electronics have been developed based on ultra-thin inorganic films of semiconductors and/or metals on flexible/stretchable substrates, which provide a routine for high performance flexible/stretchable devices.

Applications including transistors, circuits, sensors, electronic eyes, energy components, have been realized, which current rigid electronics cannot realize. The applications range from stretchable electronic interconnects (Lacour, Jones and Suo, et al. 2004), (Lacour, Jones and Wagner, et al. 2005), (Lacour, Wagner and Huang, et al. 2003), (Lacour, Wagner and Narayan, et al. 2006), (Wagner, et al. 2004), stretchable electronic devices (Choi and Rogers 2003), (Khang, et al. 2006), (Choi, et al. 2007), (Jiang, Khang, et al. 2007a, Jiang, Sun, et al. 2007), micro electro mechanical systems (MEMS), nano electro mechanical systems (NEMS) (Fu, et al. 2006), tunable diffraction and phase gratings (Harrison, Stafford, et al. 2004), (Efimenko, et al. 2005), to force spectroscopy in cells (Harris, Wild and Stopak 1980), biocompatible topographical matrices for cell alignment (Jiang, et al. 2002), modern metrology methods (Stafford,

Harrison, et al. 2004), (Stafford, Guo, et al. 2005), (Stafford, Vogt, et al. 2006), (Wilder, et al. 2006) and methods for micro/nano-fabrication (N. Bowden, W. T. Huck, et al. 1998), (N. Bowden, W. T. Huck, et al. 1999), (Huck, et al. 2000), (Sharp and Jones 2002), (Yoo, et al. 2002), (Schmid, et al. 2003).

Of many techniques, transfer printing represents one of the most effective methods to manufacturing such flexible/stretchable devices. Particularly, mechanical buckling of thin films enables mechanical stretchability. After printing stiff thin films onto a pre-strained substrate, relaxing the pre-strain on the substrate leads to buckled patterns in the stiff thin films with well defined wavelength and amplitude. Currently, 1-D configurations such as ribbons, lines or wires, have been successfully integrated for stretchable devices. It is worthy to mention that these 1-D elements were critically aligned along the pre-strain direction on the compliant substrate. For more complicate thin film based configurations, such as networks, mappings, it is inevitable that angle misalignment exists between the devices and pre-strain directions. The study of mechanics of the misaligned silicon films on a PDMS substrate helps to pave a way for developing more complex stretchable devices. Here we primarily study the angle effect on the wavelength, amplitude and buckling profile of buckled thin ribbons on compliant polydimethylsiloxane (PDMS) substrate.

1.1 Outline

The report is structured as follows. Chapter 2 discusses the different mechanics models defined. Chapter 3 discusses the experimental study and the mechanics background for the problem under consideration. It studies the effect

of angle and the width of the silicon film. The results have been discussed in terms of wavelength and amplitude and the buckling profile. Chapter 4 discusses the different modeling aspects of the finite element models created, precisely how a model has been created and the different dimensional and material parameters used. The straight case results are discussed in chapter 5. The angled case is discussed in chapter 6. The results have been discussed for change of different parameters like length, width, mesh density etc., with the change in parameters like width and angle of the stiff film. Different methods used, parameters changed to converge the results have been discussed. The chapter 7 discusses the summary of the results and future work.

2 LITERATURE REVIEW

Several approaches have been used to deposit the stiff films on the elastomeric substrates involving strong bonding of the films to the substrates at all points through the interface. The first one with sinusoidal wave patterns and networks of micro/nano-cracks is obtained by depositing metals on an elastomer (N. Bowden, W. T. Huck, et al. 1998). Second is to obtain well controlled sinusoidal geometries by transfer of solid films or ribbons created on a separate growth substrate onto the elastomer (Khang, et al. 2006)(Choi, et al. 2007) (Jiang, Khang, et al. 2007a). The procedure has been able to produce ordered buckling films with a wide range of materials including most brittle materials like single crystal Silicon and Gallium Arsenide (Khang, et al. 2006) without micro-cracks. There is another class of spatially modulated adhesion through lithography patterned surface especially for flexible electronic interconnects has been discussed in (Sun, et al. 2006)(Jiang, et al. 2007). The buckling of the film in controlled geometries involving intimate mechanical contact at the adhesion site and physical separations in the other regions. Thermal or mechanical methods are used to stretch the elastomeric substrate, prior to the deposition or transfer of the stiff film such that the relaxing pre-strain in the substrate yields a uniform compressive strain in the thin film, leading to the ordered buckling profile in turn releasing the compressive strain.

Mechanics models have been developed to understand the underlying physics of these systems (Huang and Suo 2002b)(Huang, Yin, et al. 2002) (Huang, Hong and Suo 2004). The primary goal of these is to identify the

relationship between buckling profile (wavelength and amplitude) and other material parameters and strain. The buckling profile is critical in many applications like the wavelength and amplitude play a very important role in flexible electronics, since they are related to maximum stretchability. Several non-linear analyses have attempted to calculate wavelength and amplitude of sinusoidal wrinkles (Chen and Hutchison 2004). The different buckling patterns formed due to anisotropy of membrane forces have been studied (Huang, Hong and Suo 2004), (Huang, Hong and Suo 2005). Modulus of substrate (and stiff film) plays an important role in the critical membrane force when wrinkled stiff film remains bonded to the surface. Above a critical load the wavelength of the individual wrinkles (stripes, herringbones and labyrinths) has been shown to remain unchanged with an increment in the amplitude of load (Ohzono and Shimomura 2004).

A case of Silicon film of infinite width bonded to a PDMS substrate with sinusoidal wrinkles has been considered. The displacement field is approximated to be of the form Equation 1 where A is the amplitude and k is the wave number. Shear stress at the interface is taken to be zero. Due to the application of the pre-stress parallel to the direction of the film the stresses in the membrane are accounted to be uniform. Membrane energy, bending energy of the film and the energy in the substrate form the total energy of the system.

$$w = A\cos(kx_1) \qquad 1$$

The energy of the system reaches a minimum as $\left|N_{11}^{0}\right| < h\bar{E}_f f, A = 0,$ the film is flat. When $\left|N_{11}^{0}\right| > h\bar{E}_f f,$ the flat film corresponds to a local energy maximum, and the energy minimizes when the film wrinkles with the amplitude given in Equation 2, defining the critical membrane force, $N_c \equiv h\bar{E}_f f_{\min}$, where $f = \frac{(kh)^2}{12} + \frac{g\bar{E}_s}{(kh)\bar{E}_f}$.

$$A = \frac{2}{k}\sqrt{\frac{\left|N_{11}^{0}\right|}{Eh} - f} \qquad 2$$

The minimization of the total energy with respect to both wave number k and the amplitude to get

$$\lambda_0 = 2\pi h\left(\frac{\bar{E}_f}{3\bar{E}_s}\right)^{\frac{1}{3}} \qquad 3$$

$$A_0 = h\sqrt{\frac{\varepsilon_{pre}}{\varepsilon_c} - 1} \qquad 4$$

$$\varepsilon_c = \frac{1}{4}\left(\frac{3\bar{E}_s}{\bar{E}_f}\right)^{\frac{2}{3}} \qquad 5$$

ε_c is the critical buckling strain or the minimum strain needed to induce buckling. $\bar{E}_s = E_s/(1-\nu_s^2)$ and $\bar{E}_f = E_f/(1-\nu_f^2)$ are the plane strain moduli of the substrate and the stiff film respectively.

The critical assumption behind these results is that the thin-film width is much larger compared to the wavelength involved and a plane strain assumption holds good only in this case. Otherwise, the width of the thin film also has to be

taken into consideration (H. Jiang, et al. 2008). A thin film with a width of W deposited on a compliant substrate is considered. The calculation of the amplitude and wavelength are given by minimization of potential energy in Equation 6 and Equation 9 respectively.

$$A = \begin{cases} \frac{2}{k}\sqrt{\varepsilon_{pre} - F} & F < \varepsilon_{pre} \\ 0 & F \geq \varepsilon_{pre} \end{cases} \qquad 6$$

$$\text{Where } F = \frac{\pi W \bar{E}_s}{4hE_f \rho(Wk)} + \frac{1}{12}h^2k^2 \qquad 7$$

$$k = \frac{1}{h}\left(\frac{3\bar{E}_s}{E_f}\right)^{1/3} f\left[\left(\frac{\bar{E}_s}{E_f}\right)^{1/3}\frac{W}{h}\right] \qquad 8$$

where f is a non-dimensional function of its variable. The wavelength is approximated as

$$\lambda = 2\pi h\left(\frac{E_f}{3\bar{E}_s}\right)^{1/3} \tanh\left\{\frac{16}{15}\left[\left(\frac{\bar{E}_s}{E_f}\right)^{1/3}\frac{W}{h}\right]^{1/4}\right\} \qquad 9$$

The above models predict wavelength to be independent of the pre-stress applied. However, the experimental analysis shows an approximate linear decrement in the wavelength with the increment in the pre-strain applied with a pre-strain application of 20%. A buckling theory accounting for finite deformation and geometric non-linearity has been defined (H. Jiang, D. Y. Khang and J. Song, et al. 2007). The wavelength change with the change in the pre-stress is defined by Equation 10.

$$\lambda = \frac{\lambda_0}{(1+\varepsilon_{pre})\left(1+\xi\right)^{\frac{1}{3}}} \qquad 10$$

The λ_0 is the wavelength according to Equation 3. For small pre-strains, the value of λ becomes λ_0, retaining the same variation with ε_{pre} down to pre strains close to the critical strain. The constitutive model of the substrate plays a relatively minor role on the pre-strain dependent wavelength and amplitude. The numerical models created use finite deformation instead of large deformation theory. Thus, the wavelength obtained using the numerical method is usually taken as the λ_0 and the corresponding wavelength is calculated in each case and compared with the experimental or theoretical values. The above mechanical models have discussed a situation where the silicon films are transferred onto the PDMS such that they are parallel to the direction of application of the pre-stress. However, in practice, the alignment is usually not exactly parallel. This necessitates a study of the relation between the angle of misalignment and buckling profile achieved while considering the dimensional and elastic properties of the combined PDMS-silicon system widening the scope for different applications. An integral study of the same has been done for different widths of silicon film for angles ranging from 0° to 45° angles.

3 EXPERIMENTAL OBSERVATIONS

Specifically, an elastomer PDMS (base and curing agent at the ratio of 10:1) substrate of 1 mm thick was pre-tensioned by a custom made stretching stage and UVO treated for 150 seconds to generate hydroxyl (–OH) groups on the top surface of the PDMS layer, which is essential for thin film (Si, i.e.) transferring. Parallelly, silicon ribbons of periodically increased angles have been defined on a silicon-on-insulators (SOI) wafer by photolithography and following reactive ion etching. Thin layer based Si element arrays of different geometries are physically separated from the thick Si substrate by removing the SiO2 layer in concentrated hydrofluoric (HF) acid, as schematically shown in Figure 1 (a). Followed by air drying the Si elements, a stamp from PDMS as well is brought into conformal contact with the Si elements thus to be physically adhered by each other. Quick peeling off the stamp against the Si substrate results in the elements array attached with the stamp rather than stay on the substrate yielding a successful transfer process. In the printing step, the stamp with Si elements array is slightly brought into contact with the –OH rich surface of the cured and pre-strained PDMS, where periodical changed angles exist between the ribbons and the pre-strain. Due to the competing fracture mechanisms between the interfaces of the PDMS stamp/Si and Si/cured PDMS, the PDMS stamp is be slowly peeled off without damaging the Si elements bonded with cured PDMS, since the interfacial chemical bonding between the Si/cured PDMS is much stronger than the physical adhesion between the interfaces of the PDMS stamp/Si. Finally, slowly removing the pre-strain spontaneously creates buckled ribbons Figure 1 (c)

The experiment results shows that for narrow ribbons whose width is 200um or less (10 um, 25 um, 100 um), periodic buckling waves perpendicular to the ribbon length direction rather than the pre-tension direction of PDMS appear, and their wavelengths are almost the same of 48 um after releasing the 20% pre-strain, regardless of different angles. For wide ribbons, such as 400um, apparent transitions of buckling can be seen. Near the edges, the buckling waves are inclined to be perpendicular to the ribbon direction while the middle region the buckling wave prefers orthogonal to the pre-strain direction.

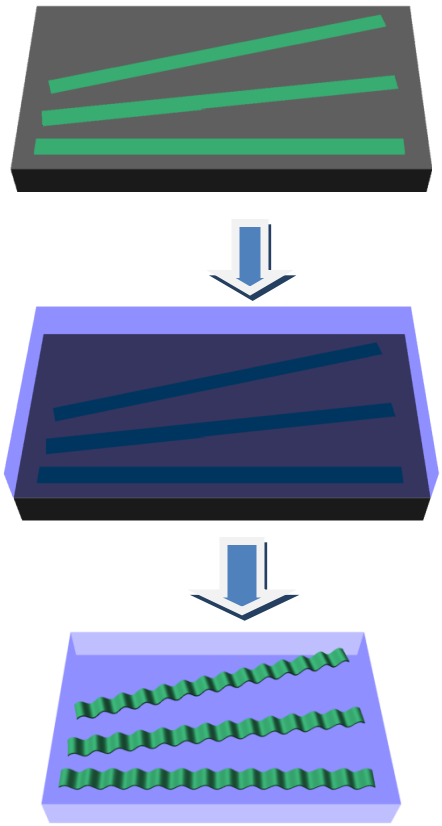

Figure 1 (a, b, c) Schematic diagram of the procedure followed

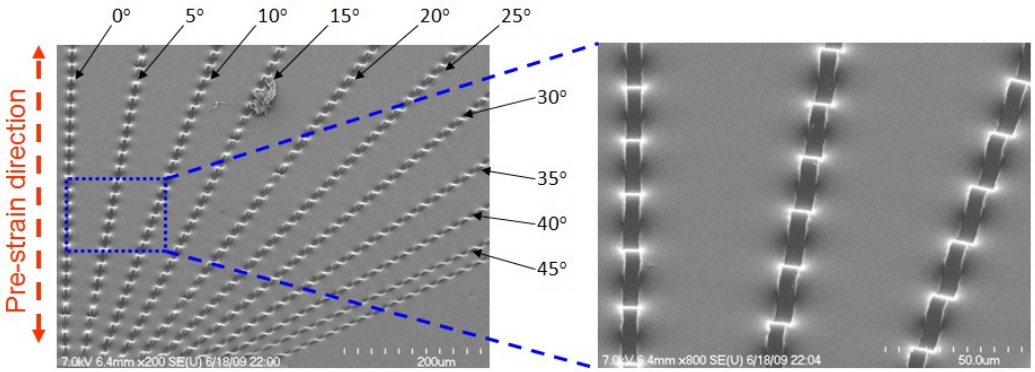

Figure 2 Pre-strain direction and results for a 10μm wide Silicon film case

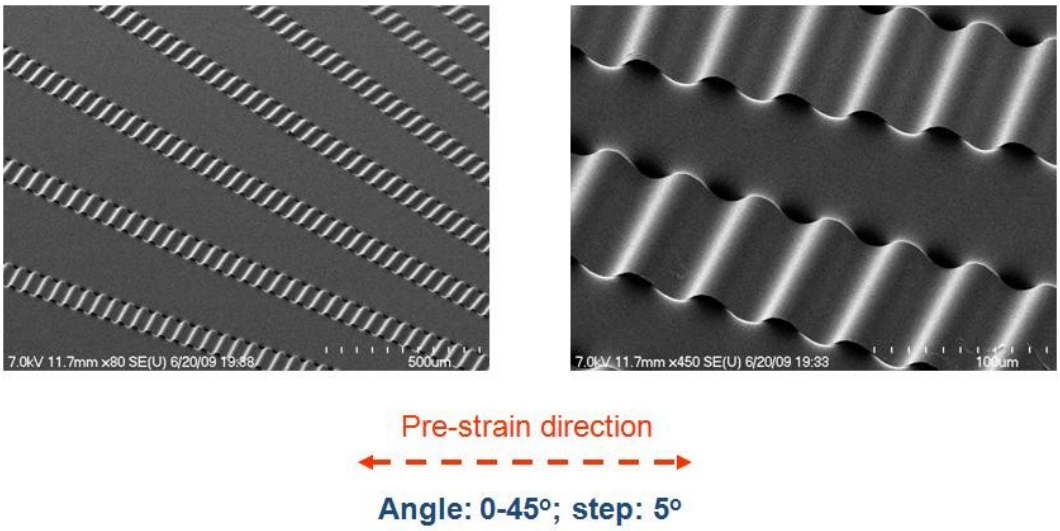

Figure 3 Results for a 100 μm case

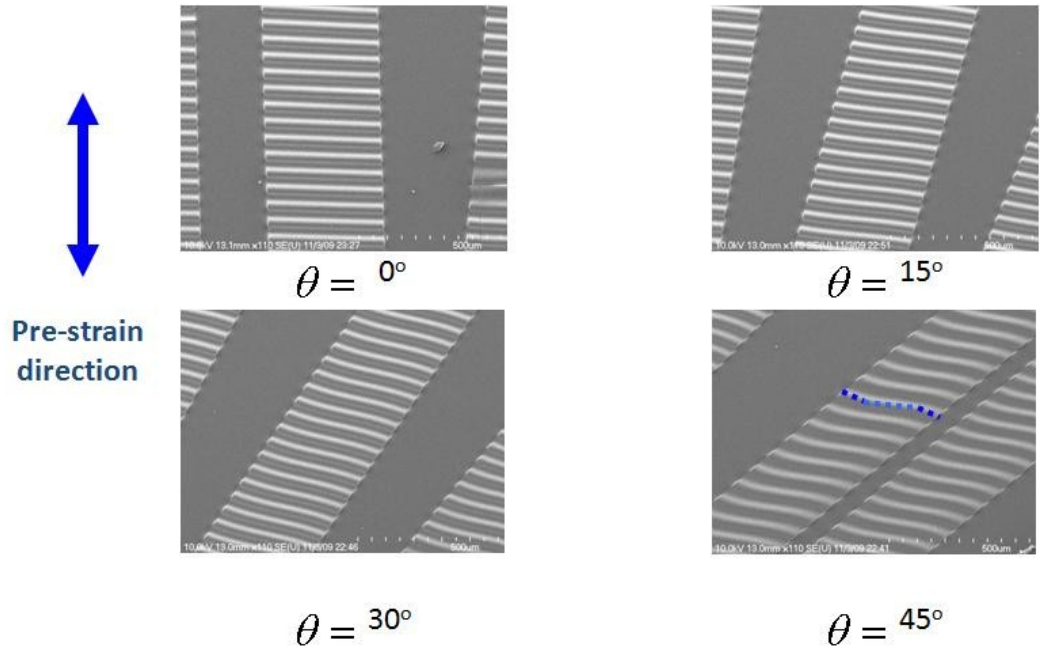

Figure 4 Results for a 400 μm case for different angles

Mechanics model

An understanding of the underlying physics of the system is very important to lay a basic foundation in order to exploit this bucking behavior. The release of the pre-strain in PDMS applies a compressive load on the Silicon. The buckling of the silicon film is due to the compressive stresses developed in the membrane. This stress is observed to be unidirectional and in the same direction as the applied stress in a 0 angle case (referred to as the straight case) and is independent of the width of the stiff film. The main assumptions used to provide a mechanics model for a zero angle case was that the stresses in the top surface are uniform, and no shear stresses are present. However, in an angled case the stresses are not uniform and do depend on a lot of factors like the angle included and the distance from a traction free edge. The stresses applied by the PDMS substrate on the silicon are not dominated by the compressive load as the case before. The

stresses are applied at an angle of 45° on each element, compressing the element as shown in the Figure 5

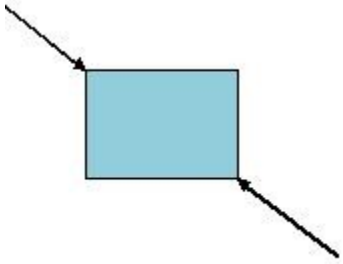

Figure 5 Stresses applied on an element in 45° angled case

In the case of a narrow Silicon film a traction free boundary condition exists at the two edges of the Silicon film, dissipating all the stresses perpendicular to the direction of the silicon film. This results in a uniaxial compressive stress state in the film. These compressive forces build up until the critical stress is reached, resulting in the buckling to occur in a direction perpendicular to the film. The same has been observed in the results of the straight and angled cases in the above experimental specimens, including narrow Silicon films (< 400 μm).

With the increase in the angle in the case of a wider film the traction free boundary condition is seen to dominate at the edges of the film resulting in the same stress conditions as described in the previous case. The buckling profile in the region where the traction free boundary condition plays a very important role is found to be perpendicular to the direction of the film. The region in the middle where the stresses due to the compressive forces created by the release of the pre-strain seem to dominate, the buckling profile is seen to align itself perpendicular

to the direction of the pre-strain. This is shown in the results above for 400 μm case.

4 MODELING ASPECTS

4.1 Finite Element Analysis

Finite element analysis is used to simulate the buckling of the Silicon stiff films and validate the results of the experimental analysis. The procedure of the application of the pre-stress is defined both by a tensile load on PDMS and the release of the same or just a compressive force on the assembly of PDMS and Silicon. The results obtained for different parameters are compared to get the minimum energy configuration for the set of results obtained. The objective of modeling is to arrive at a relation between the width of the Silicon stiff film and the alignment of the buckling profile and the wavelength when an angle is included between the application of the pre-strain and the direction of the stiff silicon film.

4.1.1 Introduction

The finite element method involves finding an approximate finite element solution for the different factors like displacements, deformations, tractions etc., on a body when subjected to a certain loading condition. It is a numerical approximation is based on an integral-differential equation called the virtual work principle given in equation which is a transformed form of partial differential equilibrium equation.

$$\sigma_{ij,j} + f = 0 \qquad 11$$

$$\int_V \left[\sigma_{ij,j} + f \right] \cdot \delta v dV = 0 \qquad 12$$

The virtual work principle is again transformed to arrive at a system of nonlinear equilibrium equations represented in the form.

$$F^N\left(u^M\right)=0 \qquad 13$$

where u^M represent the nodal variables studied. The buckling of the stiff films on a compliant substrate is a (unstable) non-linear static problem. The numerical approximation model consists of an initial linear analysis step (Eigen value buckling analysis) to provide with a geometric imperfection imported into a non-linear analysis step used to carry out the post buckling analysis.

4.1.2 Eigen Value Buckling Analysis

This analysis is used to calculate the eigen values (buckling loads) and eigen vectors of the system under consideration. The eigen value buckling analysis is based on finding the solution to the equation.

$$\left(K_0^{NM}+\lambda K_\Delta^{NM}\right)v^M=0 \qquad 14$$

K_0^{NM} represents the base state stiffness, K_Δ^{NM} represents differential stiffness, λ represents an eigen value and v^M represents the eigen vector of the system.

4.1.3 Non-Linear Analysis

The solution for a non-linear system is usually carried out by traversing the non-linear load-displacement equilibrium curve in several increments. Each increment has a set of iterations being used to arrive at the solution of the system at that particular increment. The increment size is based on the non-linear analysis

technique used. The basic equation solved for iteration in any non-linear analysis is given by equation 15.

$$F^N\left(u_i^M\right)+\frac{\partial F^N}{\partial u^P}\left(u_i^M\right)e_{i+1}^P=0 \qquad 15$$

Approximates of nodal variables are u_i^M at ith iteration and e_{i+1}^M represent the difference between this solution and exact solution.

Two different non-linear methods of analysis namely Newton's method (local buckling problem) and modified RIKS algorithm (global buckling problem) to compare the results.

4.1.3.1 Newton Raphson Method

This provides with a solution for a local buckling problem by introducing an automatic mechanism used to stabilize unstable quasi-static problems through the addition of volume-proportional damping to the model. This is attained by adding a viscous force of the form equation $F_v=cM^*v$ added to the global equilibrium Equation 15.

$$P-I-F_v=0 \qquad 16$$

P represents the external applied loads, I represents the internal loads, v is vector of nodal variables, c is the damping factor and M^* is the artificial mass matrix calculated with unity density.

4.1.3.2 Modified RIKS algorithm

The modified RIKS algorithm is based on finding a load proportionality factor in each increment of the analysis. Consider a point on the equilibrium path $A^0 = \left(u_0^N : \lambda_0\right)$. The tangent stiffness K_0^{NM} is formed and used to solve

$$K_0^{NM} v_0^M = P^N \tag{17}$$

$$\Delta\lambda_0 = \frac{\pm\Delta l}{\left(v_0^N v_0^N + 1\right)^{1/2}} \tag{18}$$

The change in λ (increment size) representing the load proportionality factor is calculated in the following manner in each step. Δl is the chosen path length which is adjusted is based on the convergence rate.

4.2 Modeling Aspects

One of the finite element models used to calculate the numerical results is shown in the Figure 6

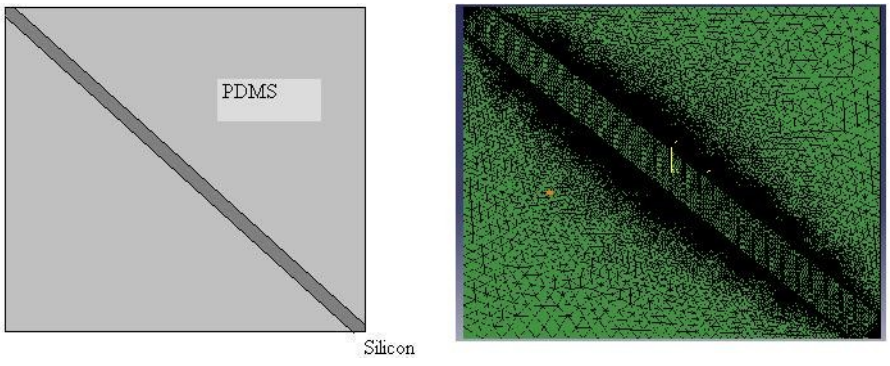

Figure 6 Numerical Model of the angled case

4.2.1 Geometric and Material Parameters

Due to the limitation of the cost of analysis, it is very difficult to create a model with the original dimensions; a part of the specimen representing the entire

model is selected. The dimensions and the other parameters are selected according to the convergence of the results of the numerical model. The analysis has been carried out for widths of stiff film ranging from 5 μm to 400 μm, with different angles included between the direction of the application of the pre-stress and the orientation of the stiff film (Silicon). The material modulus parameters used in the system are listed in the Table 1.

Table 1 Material properties of PDMS and Silicon

Material Parameter	PDMS	Silicon
Young's Modulus	2 M Pa	130 G Pa
Poisson's Ratio	0.49	0.3

4.2.1.1 Elements

The different elements used in the substrate are C3D8R (first-order hexahedral brick element), C3D20R (second order hexahedral brick element), C3D4 (tetrahedral element). The different elements used to define the stiff Silicon film are S3R (first order triangular shell element), S4R (first order quadrilateral shell element), S8R (second order quadrilateral shell element), C3D8R (first order hexahedral brick element), C3D20R (second order hexahedral brick element) to validate the results. Mainly S4R elements are used in most of the models for Silicon film due to reasons described in the next few sections. The silicon film is modeled using both brick and shell elements, but only the results with the shell elements have been mentioned in the study due to the easy convergence and lesser cost of calculation.

4.2.1.2 Interaction Properties

The interaction between the PDMS and Silicon is defined by defining two different types of constraints. One is the nodes at the interface of the film and substrate is merged such that the nodes move together under the application of load on the substrate. In order to obtain this the number of nodes at the interface on the substrate has to be exactly the same as the stiff film. The other one is a tie constraint defined between the surfaces of substrate and film at the interface. The number of nodes on the substrate and the film depend on the type of tie constraint used. It is better to maintain the same number of nodes and defining a node to node tie constraint. To attain the different mesh densities on PDMS sections are defined with seeds defined on the edges.

4.2.1.3 Mesh Density

The mesh density in the Silicon is maintained in a range of 1μm/element to 10μm/element for mesh sensitivity analysis. The optimum mesh density of the silicon film is found to be 2 μm/element for the all the models, such that there are at least 20-25 elements in each wavelength. The mesh density of the PDMS substrate ranges from the same as the silicon at the interface to 200 μm/element.

4.2.1.4 Loading pattern

The tensile stress on the PDMS applied in the experiment is modeled using three different types of loading conditions.

- Boundary conditions applied as a uni-axial tensile or compressive load on PDMS by applying a displacement boundary condition on sets of nodes defining the two surfaces of PDMS.

- An equation constraint (This constraints the displacement in one direction of all the nodes on the surface to be equal) defined on all the four surfaces defining the four sides of PDMS and silicon such that they move as a plane.
- Temperature has also been used to apply both normal and shear strains as loading on the PDMS. This is done by defining anisotropic thermal expansion coefficients.

The loading pattern and the number of steps involved depend mostly on the type of analysis used. The different types of analysis and the steps involved are defined in the following section.

4.2.1.5 Arc-Length Method

This section describes the steps involved, the type of load applied in Arc-length method, and how they are analogous to the experimental setup. Both first and higher order elements have been used in each case to compare the results. The different boundary conditions applied throughout the model are represented in the Figure 7.

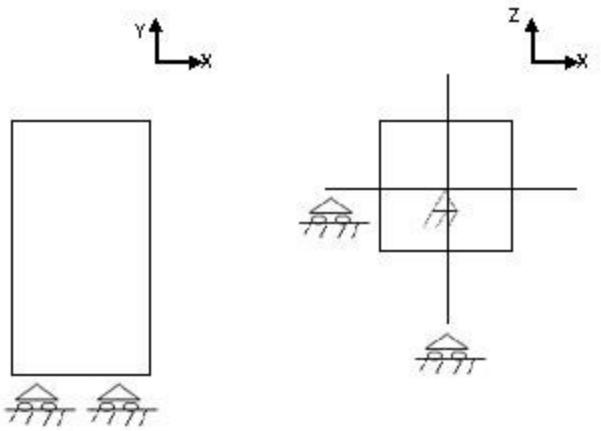

Figure 7 Boundary Conditions for Arc-Length Method

The entire analysis is carried out in seven steps involving two different methods of analysis in ABAQUS 6.7.

Step 1: The pre-stress is applied as a strain load on the PDMS by removing the elements defining the Silicon film (This is obtained by using shell elements on the stiff film which share nodes with the substrate at the interface.).

Step 2: Restore the film elements

Step 3: Mode Analysis has been carried out by applying a load which is a normal load on two of the surfaces in the direction of the pre-strain applied on the substrate to find different Eigen modes for the model.

Step 4: Observe the modes calculated, and a reasonable mode close to the experimental results is selected (a sine-shape mode is chosen). The chosen mode is imported to another file with a 1% imperfection (Element set defining the substrate is imported). The substrate is pushed back by the same amount as the pre-stress applied.

Step 5: Remove the film elements and stretch PDMS.

Step 6: Restore film elements. This ensures a wavy substrate(pre-strained) and a wavy thin silicon film(with no strain).

Step 7: Release the pre-strained applied on PDMS to generate buckling.

4.2.1.6 Newton-Raphson Method

In the Newton's method the analysis is carried out in a single step using the Stabilize option in ABAQUS. The pre-stress on the substrate is applied as a compressive displacement load on the nodes of the two surfaces of PDMS.

The different boundary conditions applied throughout the model are represented in the Figure 8

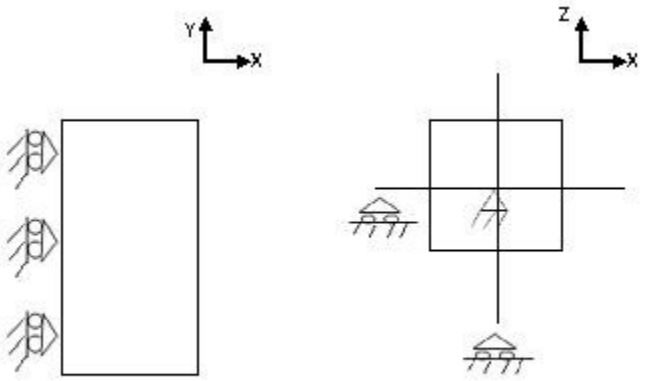

Figure 8 Boundary Conditions for Newton-Raphson Method

5 STRAIGHT CASE

The straight case is used as a validation for the results of the angled case and also helps to lay a basis for the choice of the dimensional parameters, elements, method used for the numerical approximation etc. Moreover, the straight case includes a lesser number of elements when compared to an angled case An eigen value buckling analysis is carried out on the model and a combination of the first three buckling modes are imported as an imperfection (less than 1%) and a static non-linear analysis (Newton's approach) instead of Modified RIKS method and Newton Raphson method has been used to perform the post buckling analysis. A displacement load is applied on the nodes of two sides of the substrate. The range of widths of Silicon stiff films have been modeled from 5 μm to 40 μm. The study is divided into two categories according to the ease of convergence of the results which in turn depends on the width of the stiff film. In the following numerical models, the strain load applied usually ranges from 0.1% to around 1% which is very less compared to the original experimental results.

Effect of different factors like the loading conditions, Length of the stiff film/substrate, element type, mesh density, order of accuracy has been studied. The results are compared in terms of the energy, wavelength, buckling profile and the stress distribution. An optimal length of the Silicon film has been obtained to be around a value of 15 times the wavelength. The element type, order of accuracy seems to not show any effect on the wavelength, the amplitude, the buckling profile, stress distribution, and the energy of the system.

5.1 Narrow Stiff Film

The substrate and film dimensions of the current finite element model are 2 mm (length), 2 mm (width) 0.5 mm (thickness); 20μm (film width). The buckling and the post buckling analysis show a sinusoidal buckling profile with a converged wavelength of 53 μm which is the theoretical value and experimental value according to equation 10 (due to the difference in the pre-strain). The out-of-plane displacement of post buckling results have been shown in the Figure 9. The stress distribution (S11- along the direction of the film, S22 perpendicular to the film) through the width of the film along a crest of the buckling profile is normalized are listed in Table 2.

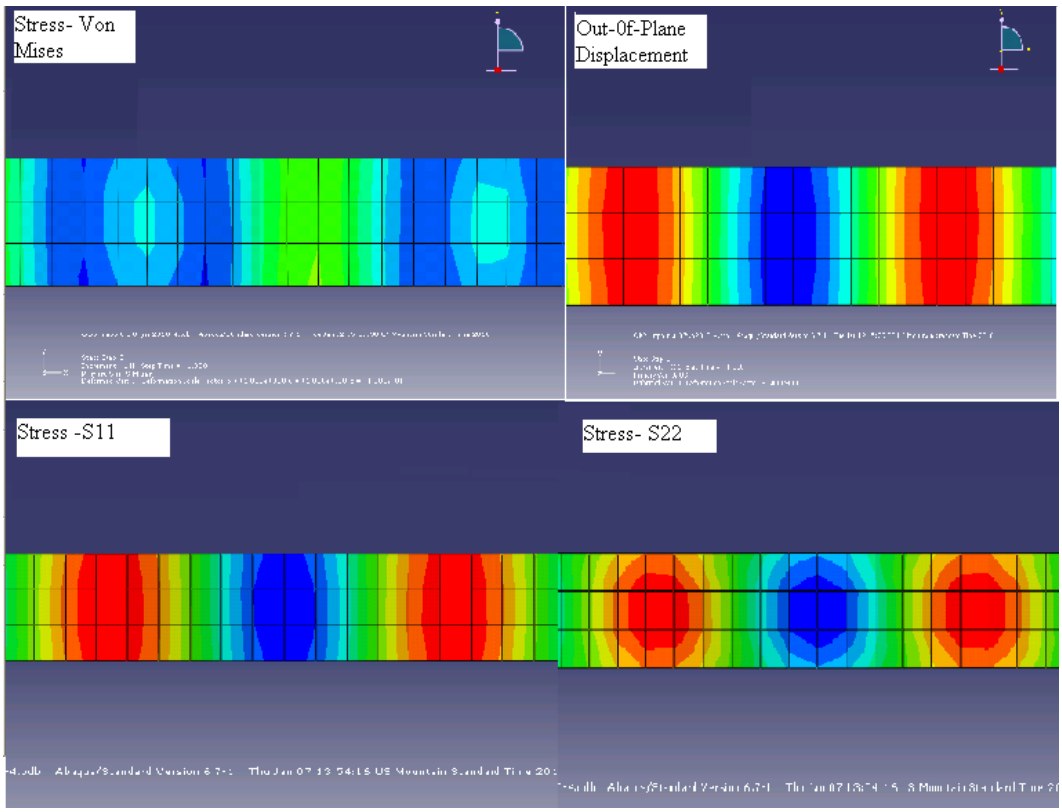

Figure 9 Stress and displacement results for a 20 μm case

The following conclusions can be drawn from the above table. A uniform compressive stress in the direction of the film is much (~5 times) higher when compared to the stresses in the perpendicular direction. The stresses perpendicular to the film are shown to decrease as they reach the traction free boundary condition at the edges of the film. This decrement in the stresses at the edges is shown to play a very important role in the results of the angled case.

Table 2 Stress Distribution for 20 μm case

	S11	S22
1	1	0.1913
2	0.998	0.2212
3	0.9934	0.1913

In order to confirm the above results a confirmation run is carried out using Newton-Raphson iteration method with the dimensional parameters of 0.32 mm x 0.1 mm x 0.1 mm (length x width x thickness of PDMS substrate) and 13.6 μm wide film. The results of the same are shown in Figure 10. The wavelength, buckling profile, stress distribution, and amplitude are observed to be the same as the previous result.

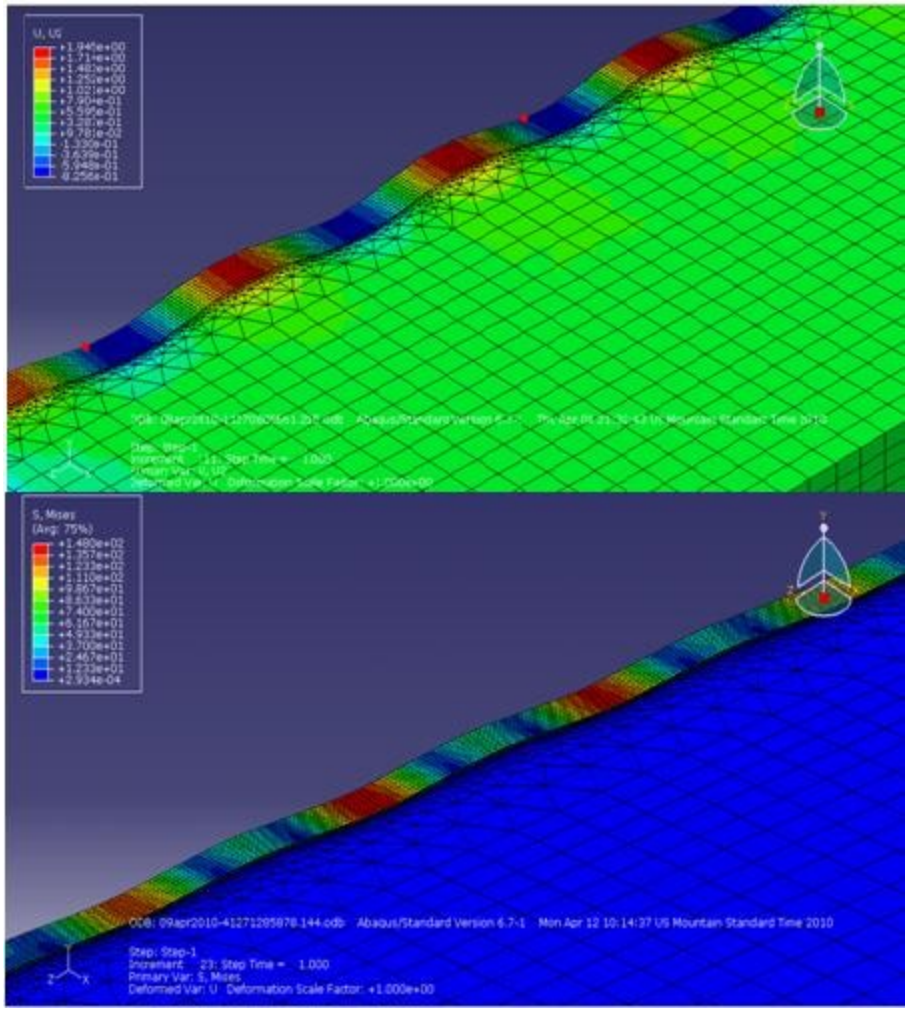

Figure 10 Post buckling results - stress and displacement for a narrow Silicon film (13.6 m)

5.2 Wide Stiff Film

The case with the wider films seems to show a (inverted cup or conical shape) combination of two sinusoidal waves perpendicular to each other and perpendicular to the stiff film direction both in the buckling and post buckling analysis as shown in Figure 11. The amplitude of the buckling profile is noticed to be very high compared to the theoretical value. The reasons for the same can be deciphered in the following manner. The wider silicon film is behaving like a

plate under buckling instead of behaving like a beam under buckling. This could be the main reason for the huge increase in the wavelength both in buckling and post buckling analyses with the increase in the width of the stiff film. This result could also be attributed to the branching of the post buckling analysis into an unstable bifurcation leading to an increment in the energy of the system.

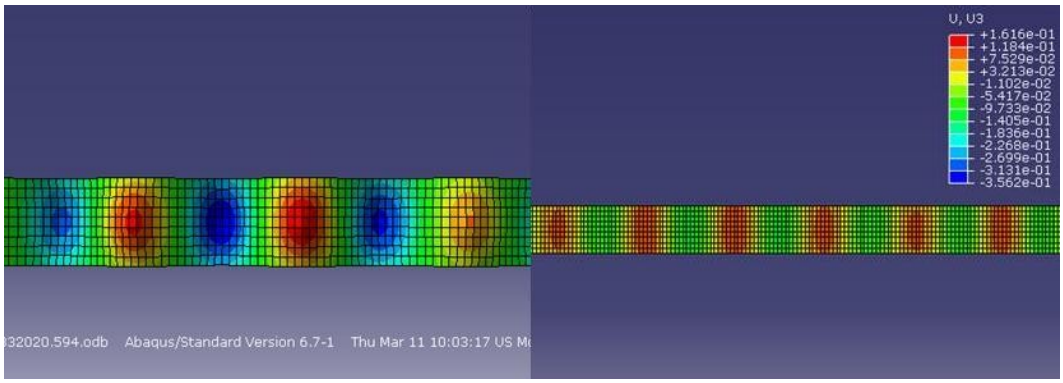

Figure 11 Buckling and post buckling results of 40 μm case

The normalized stress distribution of the post buckling results has been plotted in Figure 12. The figure shows that both the stresses are forming a sine wave providing a varying stress in the direction parallel to the silicon film, both the stresses are comparable to each other. The theoretical discussion in the chapter 2 discusses that the strains and stresses in the direction perpendicular to the film are comparatively much lower and do not play a big role in the buckling of the stiff film.

In order to find the exact solution, a study of the effect of geometric parameters like width, length and thickness of the substrate, and loading conditions has been summarized in the following sections.

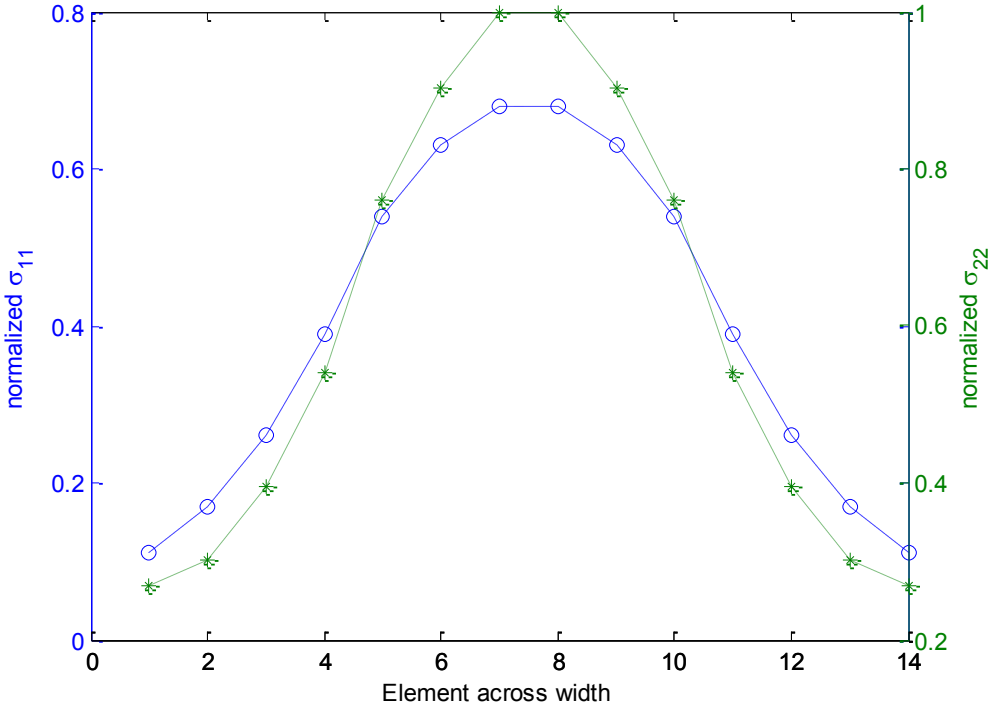

Figure 12 Plot for the stress distribution for 1600 μm case

5.2.1 Effect of Loading conditions

Two different types of loading conditions have been used to apply the pre-stress in PDMS. Method one defines a displacement load on the nodes of the two surfaces which are perpendicular to the direction of the film. The results showed a rather large edge effect as shown in Figure 13. As a result, buckling profiles and stress concentration have been notices at the edges of the model. This resulted in a failure in the elements at the edges of the film even before the region towards the center reached the critical buckling load. Method two involves using an equation constraint defined on a set of nodes at the edge (both the substrate and the film) perpendicular to the direction of the film with equal displacement in the direction of the film. A displacement load on one of the nodes is used to apply the pre-

strain in the substrate. This method showed a uniform distribution of the stresses applied throughout the simulation time from the initial increment thus resulting in a uniform buckling profile.

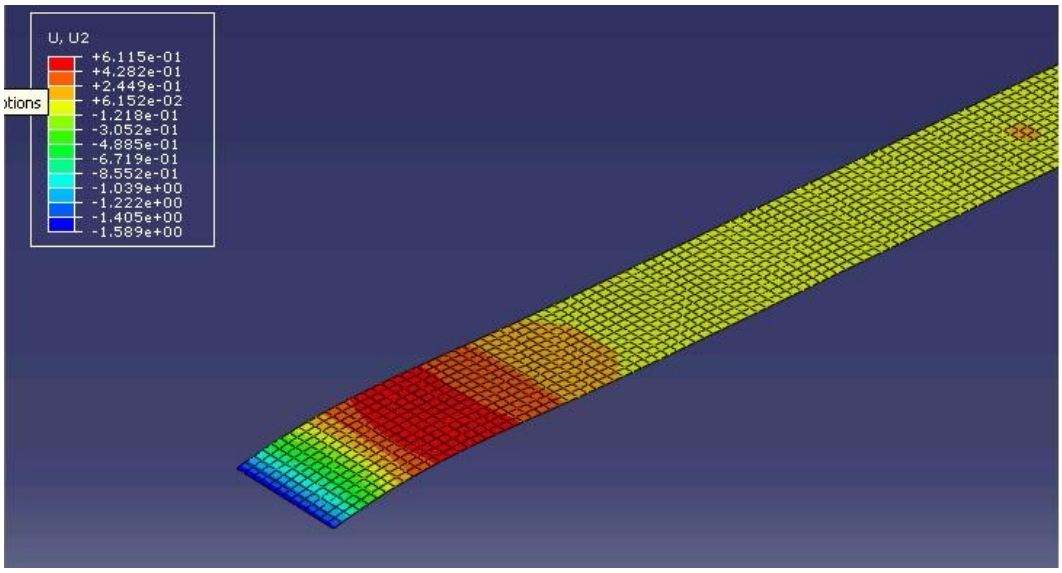

Figure 13 Post buckling results using boundary condition

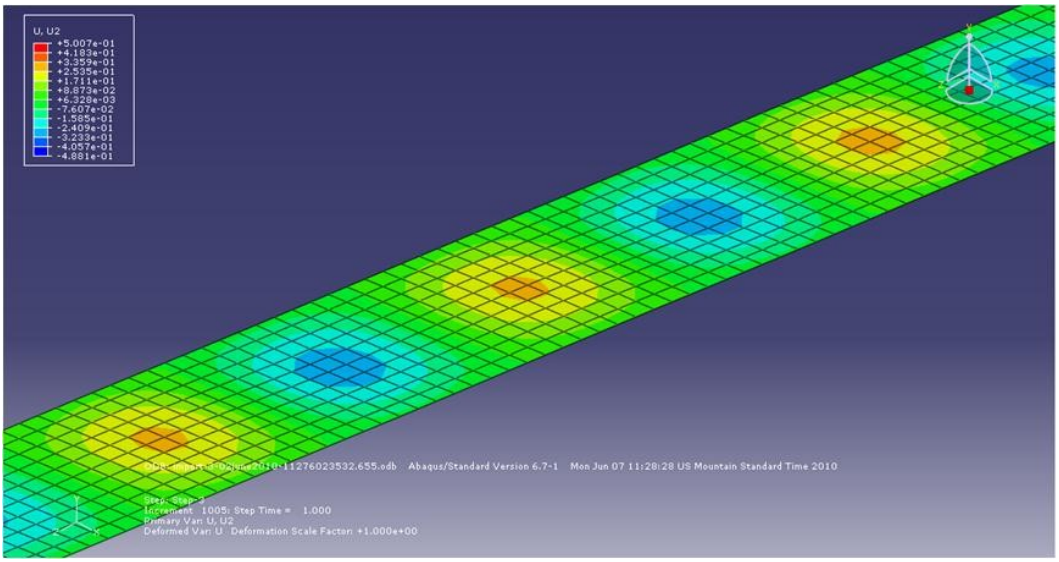

Figure 14 Post buckling results with equation constraints

5.2.2 Effect of Width of the substrate

Finite element models with different widths (substrate) cases have been numerically formulated using modified RIKS algorithm (Arc-Length method). The geometrical parameters are shown in the Table 3. Equation constraints are used to apply a pre-strain for the reasons described in the section 5.2.1.

Table 3 Geometric properties of the finite element model for 40 μm wide film

	PDMS Substrate	Silicon Film
Width	400 μm, 500 μm, 600 μm, 700 μm, 800 μm	40 μm
Length	1800 μm	1800 μm
Height/Thickness	4000 μm	340 nm

The post buckling results of the numerical models are given in Figure 16 and Figure 17. Since eigenvalue buckling analysis is a linear perturbation process the results are the same in all the cases and as the case above in terms of buckling profile and the wavelength (82 μm). However, the post-buckling analysis, which forms a good approximation for non-linear processes like buckling has shown a convergence in the results in terms of the wavelength (48 μm) and the buckling profile changed to a perfect sinusoidal wave in the 40 μm case where the width of the substrate is reduced to a value of 8 times the width of the silicon film. The results of the simulation and the theoretical, experimental results have been listed in Table 4. The normalized stress distribution along the width of the crest of the buckling profile of a case of 400 μm case is plotted in Figure 15.

The stress distribution and the displacement follow the same conical profile as discussed in the previous section. Unlike the conical buckling profile

case, for the case with the sinusoidal buckling profile the uniform uniaxial compressive stress in the direction of the pre-stress (film direction) dominates. The total energy of the system has been observed to decrease from the first numerical model to the converged result by 50% (from the table above), thus proving that the theoretical result of sinusoidal buckling profile corresponds to the state of minimum energy.

Table 4 Result discussion for different width of substrate

Results/Width of Substrate	400 µm	500 µm	600 µm	700 µm	800 µm
Wavelength	50 µm	75 µm	78 µm	82 µm	82 µm
Normalized Energy	0.545	0.82162	0.8743	0.9648	1

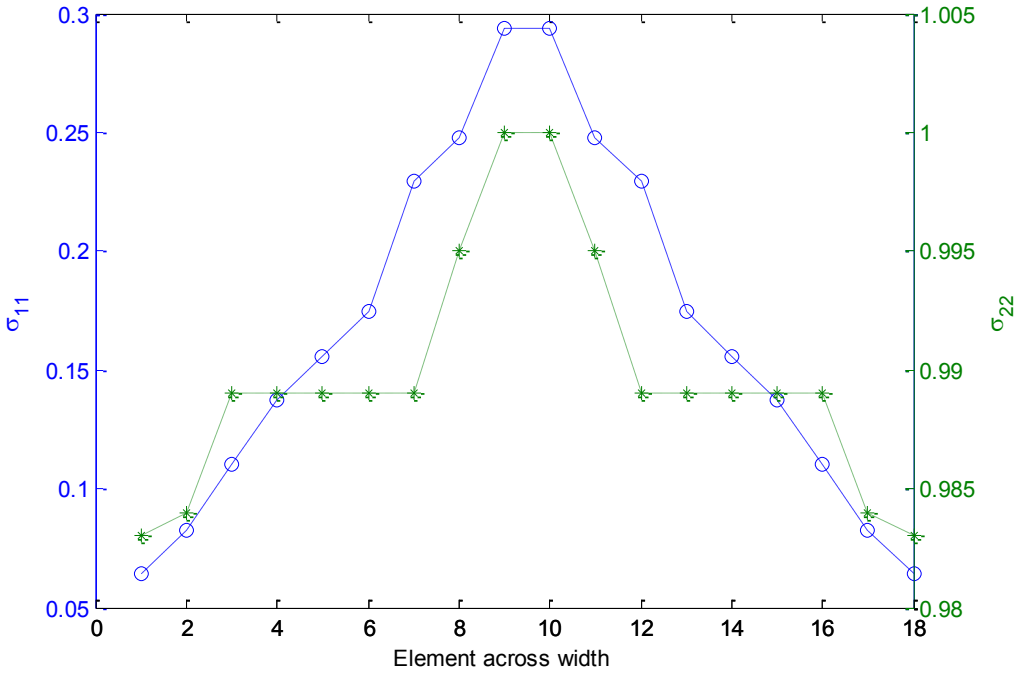

Figure 15 Plot of the stress distribution in a 400 µm case

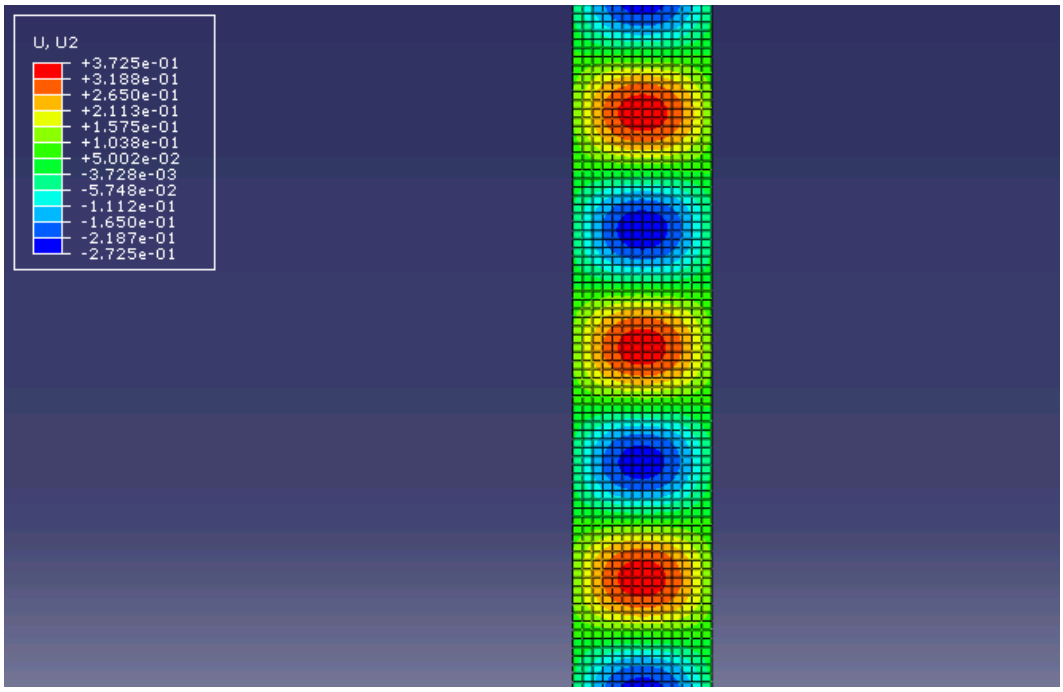

Figure 16 Post buckling results for 0.8 mm x 1.6 mm x 4 mm case

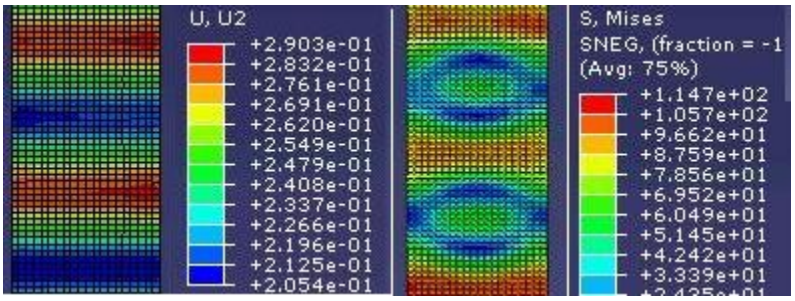

Figure 17 Post buckling results for 1.6 mm x 0.4 mm x 6 mm case

5.2.3 Newton's Approach

A model with 34 μm wide silicon layer is modeled with different dimensions to check the effect of the dimensions of the PDMS layer on the buckling wavelength and a similar dependence of the results as mentioned above on the width of the substrate has been found in the post-buckling results of the wide silicon film case. The final result has been shown in Figure 18.

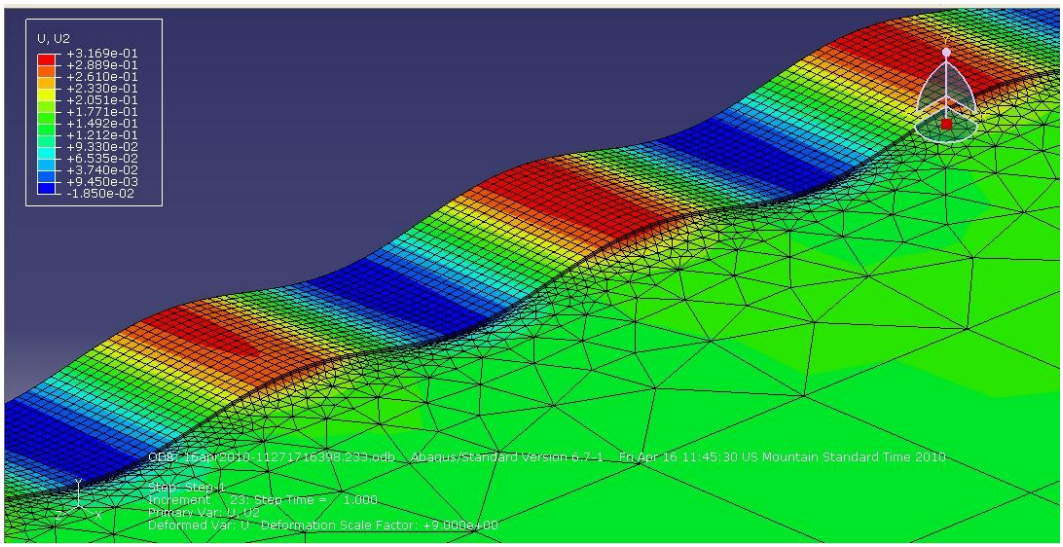

Figure 18 Newton raphson approach results for 34 μm case

Thus in the numerical approximation of the straight case, the shape of the buckling profile depends on the dimensional parameters used. It can be concluded that the length of the stiff film under consideration should be at least greater than 20 times the wavelength in order to obtain uniformity in the buckling profile. The results seem to have an edge effect which can be removed by defining equation constraints in place of normal boundary conditions on the compliant substrate. It can derived that the results of the wider stiff films easily converge with the theoretical or experimental results when the width of the substrate is around eight times the width of the stiff film for a 40 μm case. This can be supported by the fact that the spacing between the films in the experimental specimen is maintained to be 5 times the width of the stiff film.

6 ANGLED CASE

An initial numerical model for an angled case with 45° angle included has been analyzed to identify potential challenges in the convergence of the results. The geometry and the numerical model created in ABAQUS are shown in the Figure 19. The dimensional parameters used are listed in the Table 5.

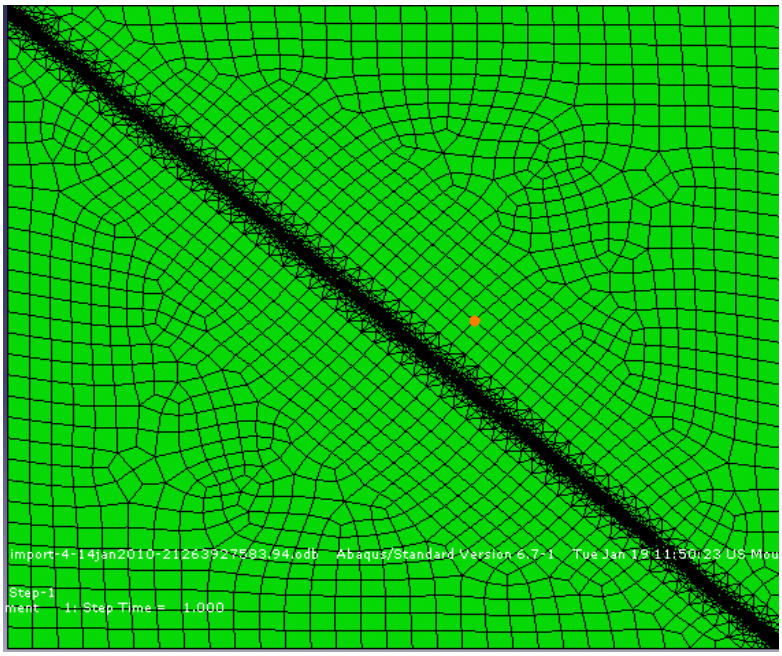

Figure 19 Initial numerical model for an angled case

The results of the post-buckling analysis of the different models are shown in the Figure 20. The theoretical wavelength has been plotted in Figure 23. The theoretical and simulation results of the wavelength for the different widths of the stiff film are seen to diverge from each other after a width of 35.8 μm model by a huge amount. The wavelength is seen to double from one case to another, the conical and comparable stress distribution (as in the case of the straight silicon film) which is not the case with the theoretical analysis results (for example for a

case of 20 μm to 40 μm wide silicon film wavelength changed from 48μm to 82 μm).

Table 5 Dimensional Parameters of the numerical models

Parameters	Silicon	PDMS
Height	340 nm	500μm
Length	2.83mm	2 mm
Width	14.2μm, 21.4 μm, 35.8 μm, 72.5 μm, 183 μm	2 mm
E	130 G Pa	2 M Pa
ν-Poisson's Ratio	0.3	0.49

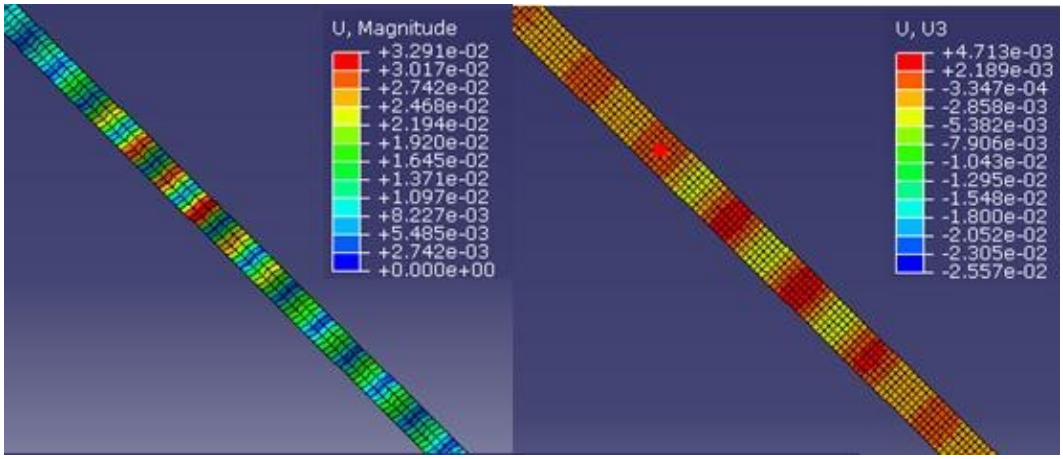

Figure 20 Post-buckling results for 14.2 and 21.4 μm respectively

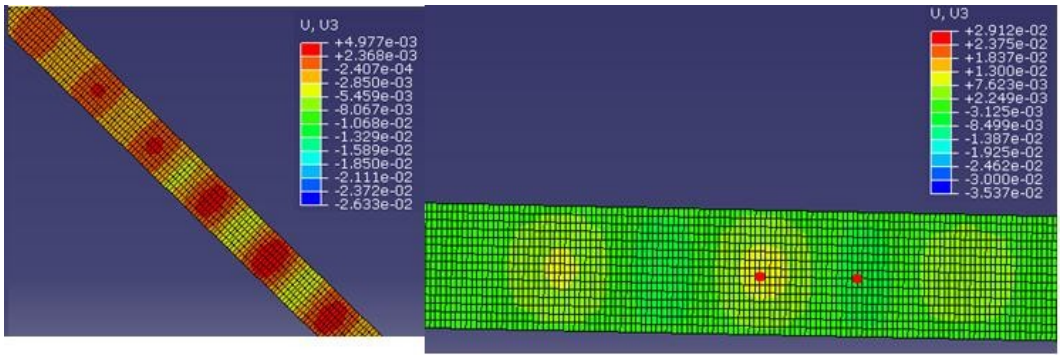

Figure 21 Post-Buckling results for 35.8 μm and 72.5 μm

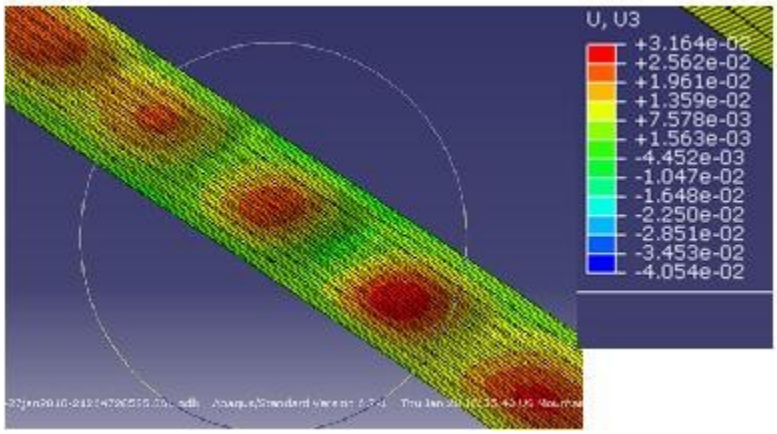

Figure 22 Post-Buckling results for 183 μm

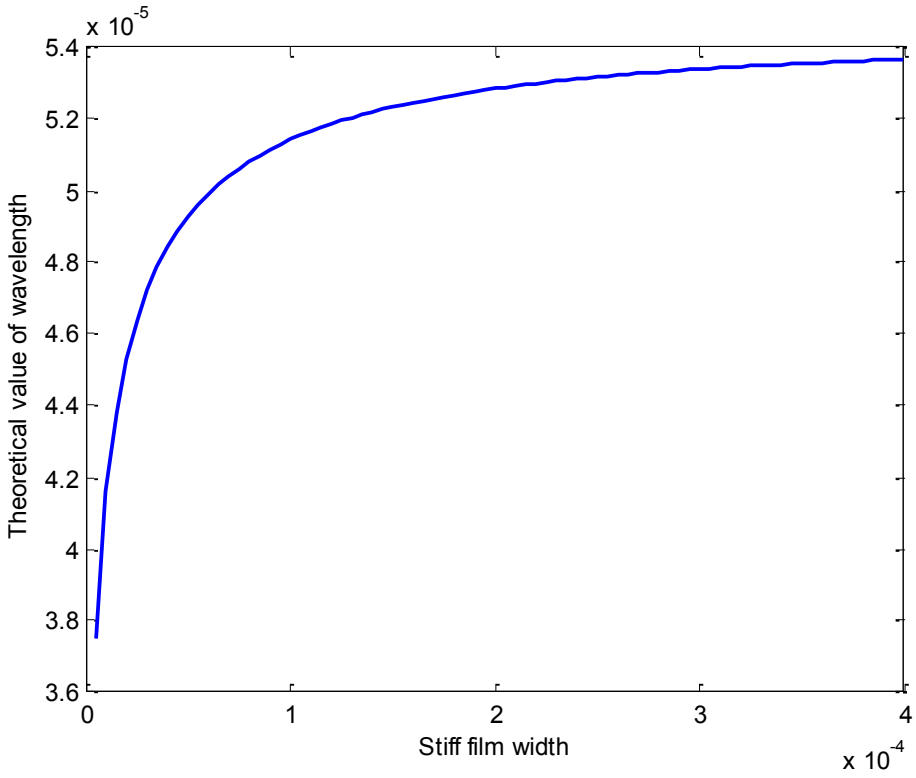

Figure 23 Theoretical wavelength Vs Stiff film width

The above results in turn help dividing the study into two different cases, a narrow silicon film (less than 20 μm) and a wide silicon film (greater than 30 μm) as in the straight case.

6.1 Narrow Stiff films

The dimensional parameters and the comparison of the post-buckling results showing the effect of length are provided in Figure 24, Figure 25. The above results show that the buckling of the model does not occur until the length of the silicon stiff film (15-20 times the wavelength) establishing a required length of the silicon film for critical buckling load to be achieved.

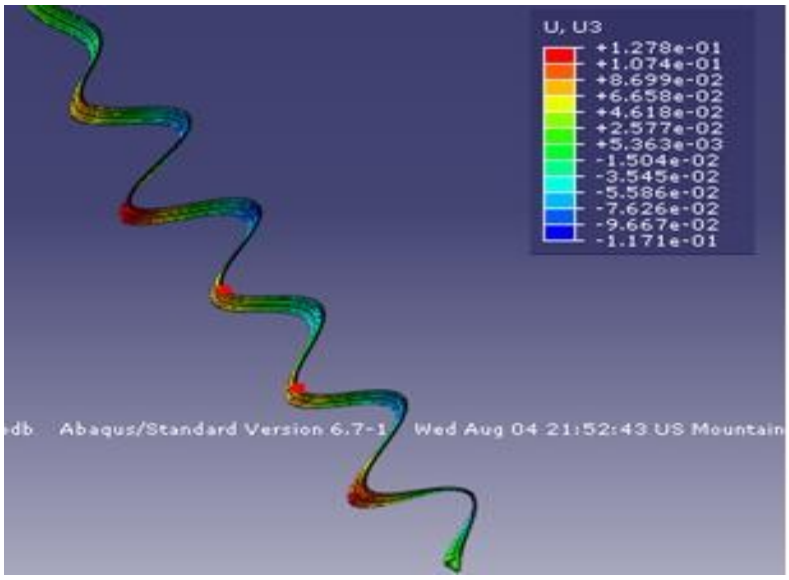

Figure 24 Post buckling analysis results (1.6 mm x 1.6 mm x 6 mm)-10 μm wide stiff film

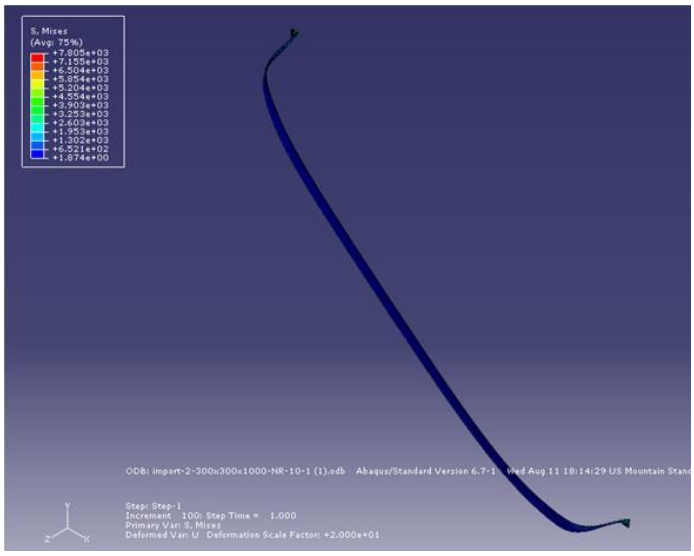

Figure 25 Post buckling results (0.3 mm x 0.3 mm x 6 mm)-10 μm wide stiff film

The effect of the type of the element on the results of an angled case for a 14 μm wide stiff film numerical model is studied using arc-length method and the post-buckling results for the same are given in Figure 26. The results do not show

change in the wavelength (47 μm) or the amplitude (0.18 μm) of the buckling profile. The total energy of the system remained the same in both cases.

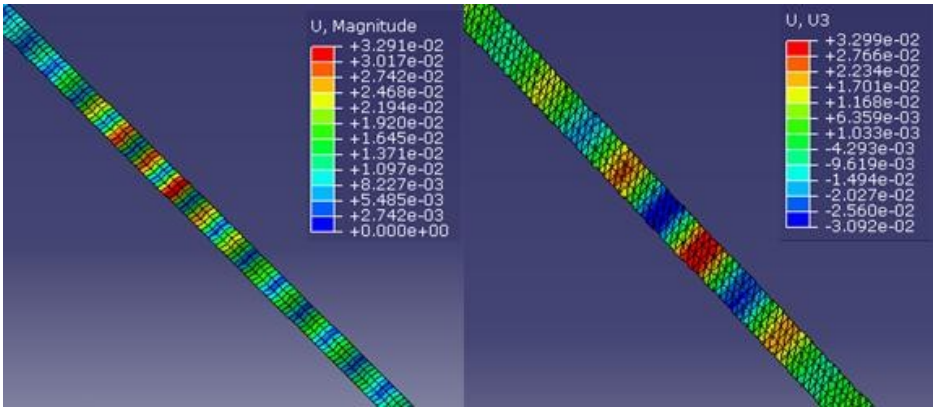

Figure 26 Comparison of results by using S3R and S4R elements on stiff film

6.2 Wide stiff film

In order to study the effect of angle on the convergence of the results a case with wider stiff film (greater than 30 μm) has been studied. A numerical model with the dimensions 1.6 mm x 0.4 mm x 6 mm substrate dimensions and 40 μm wide stiff film, with an increasing angle included between the application of the pre-stress and in steps of 1°.It is observed that the number of elements in the model increases with the increment in angle included. The maximum load that can be applied to the model has been noticed to decrease with the increase in the angle. The numerical model used is shown in Figure 27.

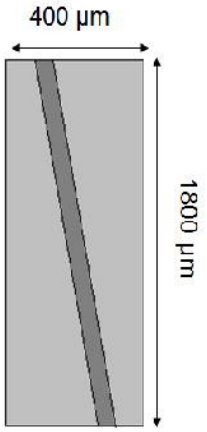

Figure 27 Numerical models for less angle case

Eigenvalue buckling analysis results in different modes with a buckling profile conical in shape and wavelength of 80 µm for all angles included. The post-buckling analysis results for both the analysis of a case of 2.5° and 5° angle has been given in Figure 28 and Figure 29.

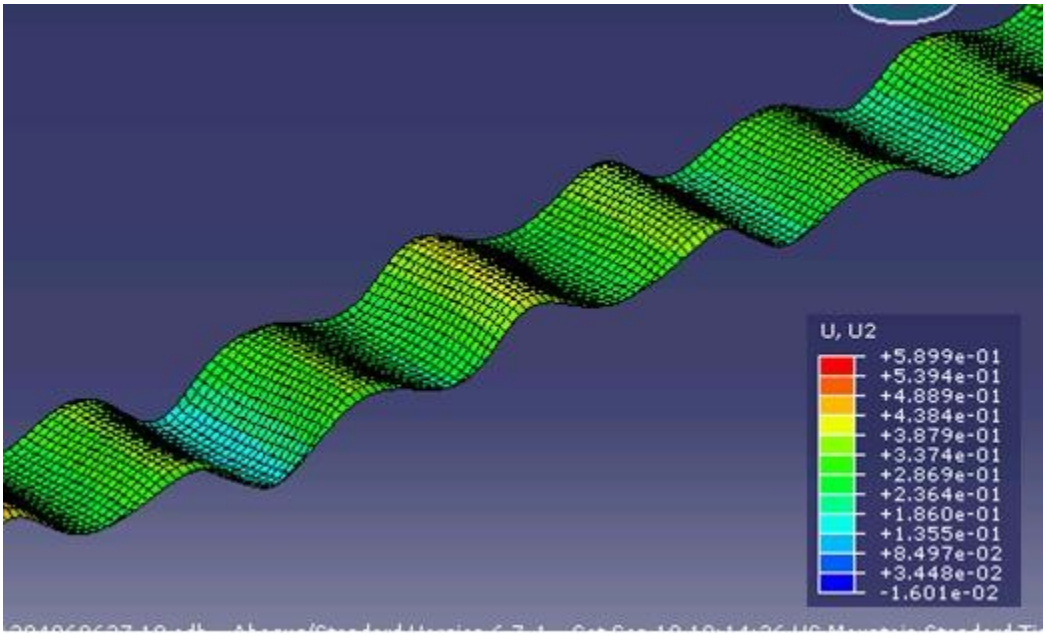

Figure 28 Post buckling result for 2.5° angled case

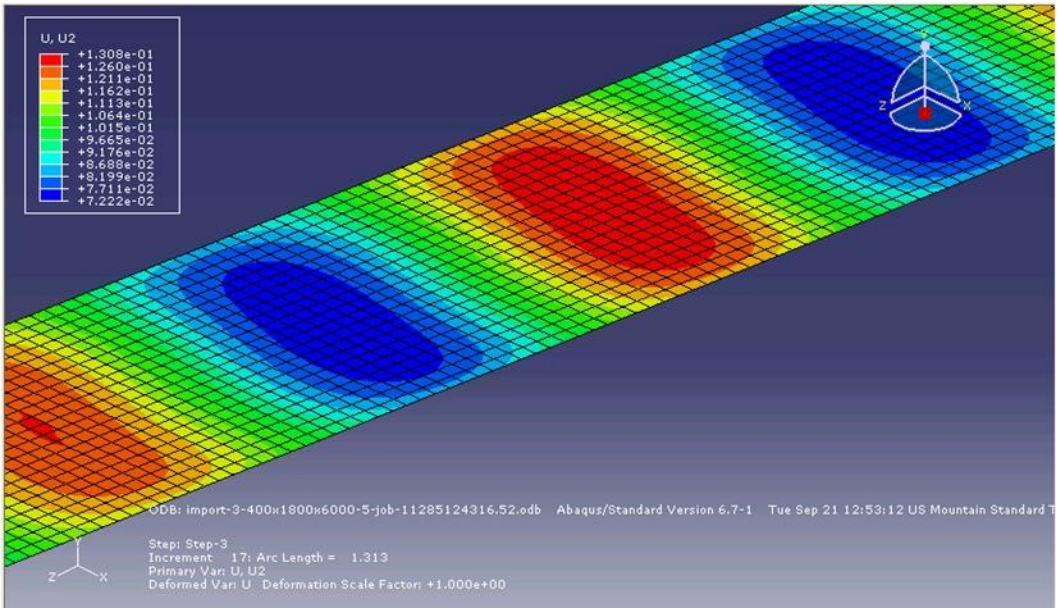

Figure 29 Post buckling result 5° angled case

The post buckling analysis results from above show a discrepancy as the included angle increased. The total energies of the system in both the cases have been compared to show that the sinusoidal wave has a lesser value and difference of 30% has been found.

6.2.1 Effect of higher angle

In order to solve this issue of the convergence of the results for the angled case greater than 5°, a 45° angle case with 40 μm has been considered. The change of a variety of parameters like higher order element formulation, order of accuracy in integration, and mesh density are found to show no difference in the results obtained. A study of the imperfection imported, and change in the dimensional parameters has been carried out as shown in the following section.

6.2.2 Effect of the Imported Imperfection

Imperfections initiate branching to a secondary path in a bifurcation problem involving buckling. This is especially useful if this path is still stable, i.e. the load can still be increased, and then imperfections are necessary for convergence. Since buckling is non-linear and the results are unstable, the imperfection imported should not impart any change in the results of the post buckling analysis. A random mode combination has been imported for the same finite element model and the results have been found to be stable. To confirm this, four different preselected geometries with an imperfection ranging from 1% to 10 % (of the characteristic length of the stiff film) have been simulated with the help of MATLAB (code used is attached in the appendix) and imported to carry out the post-buckling analysis using modified RIKS method in ABAQUS. The pre-selected geometries are with buckling profile wavelengths 40 and 80 μm perpendicular to the direction of the stiff film and the direction of the pre-strain.

There is no change in the results both in terms of the buckling profile and in terms of the wavelength, stress distribution and energy. The imperfection in the film and the results for the numerical model with imperfection (buckling profile perpendicular to the direction of pre-strain with a wavelength of 40 μm) of 10% have been shown in Figure 30 and. Figure 31

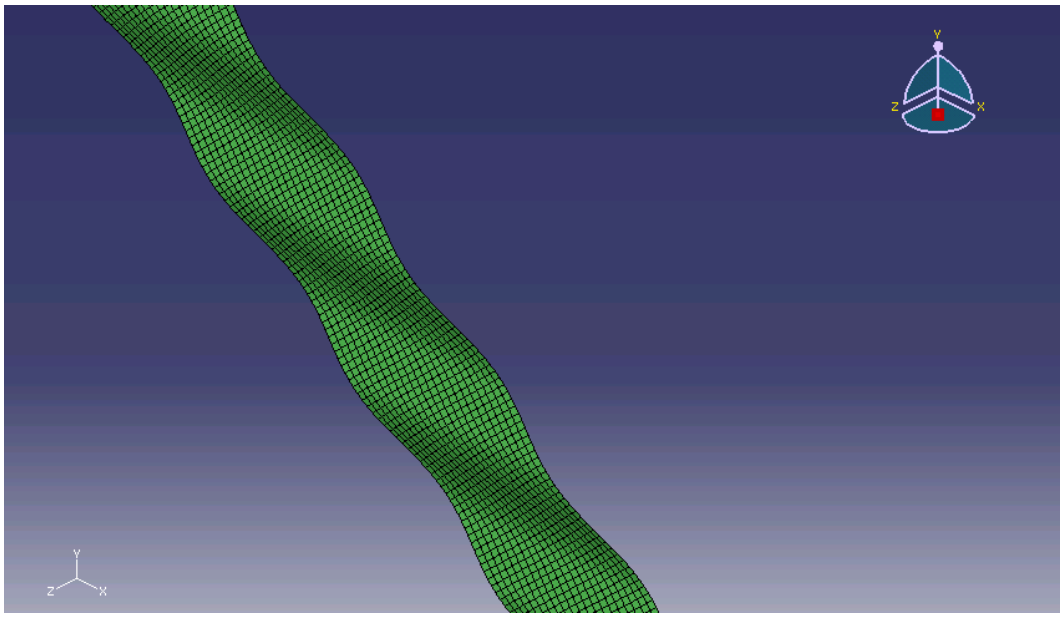

Figure 30 Initial imperfection geometry of 10%

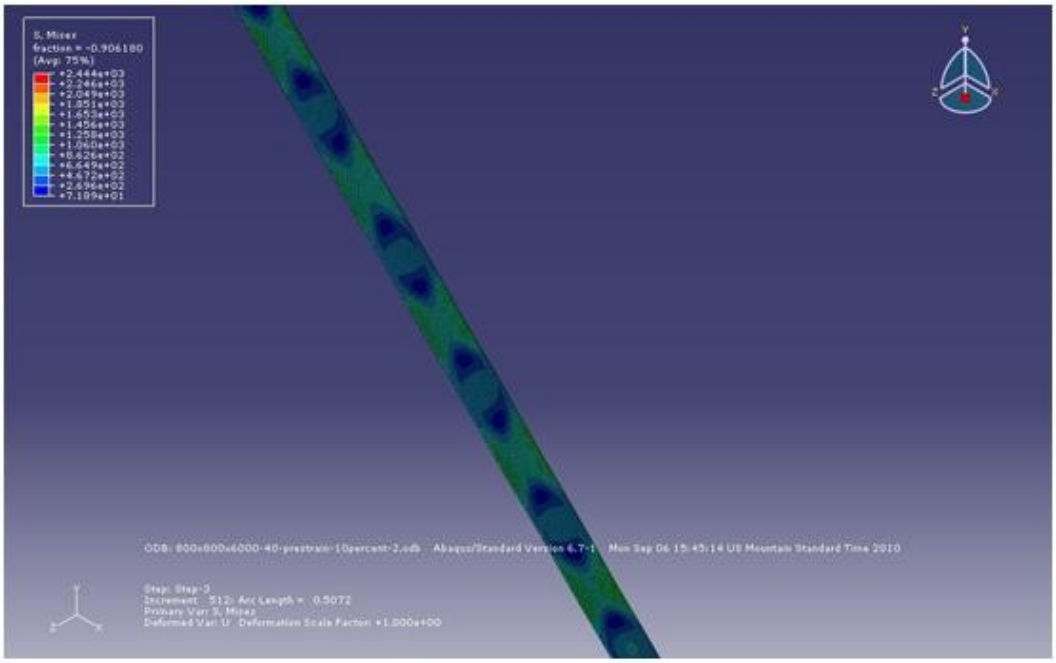

Figure 31 Stress distribution - 40 μm case- 10% imperfection imported

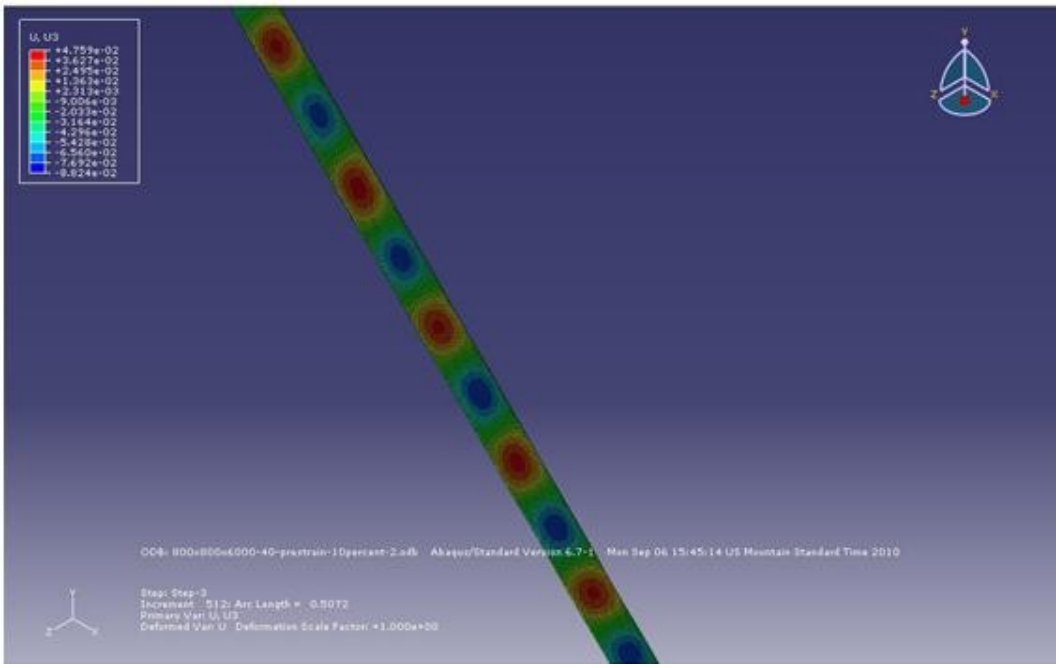

Figure 32 Out-of-plane displacements - 40 μm - 10% imperfection imported

An evident change in the direction and the shape of the buckling profile (stress distribution, displacement from sinusoidal and conical), wavelength (40 μm to 82 μm) has been observed through the increments of the release of the pre-strain in the model showing no evident change in the result from the previous cases discussed.

6.2.3 Effect of the width of the substrate

As discussed in the section for straight case, the width and its effect on the post-buckling analysis results of the angled case have been studied using geometry as shown in Figure 33 using modified RIKS algorithm.

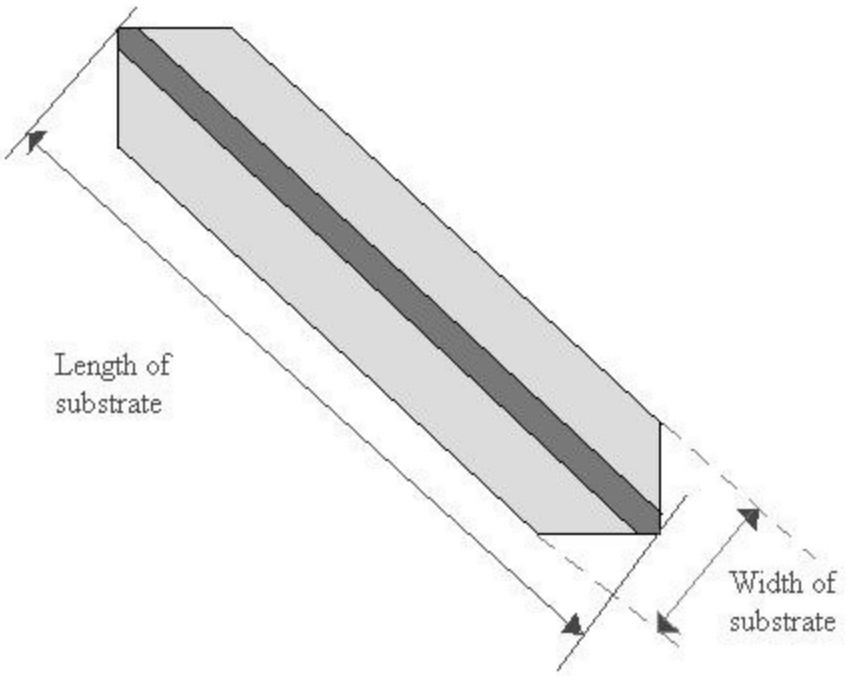

Figure 33 Geometry for a less wide substrate

In order to apply a load at 45°, an anisotropic temperature expansion coefficient has been defined on the PDMS substrate and a temperature pre-defined field is used to apply a uniaxial temperature load. The stress distributions on the crest of the buckling profile have been calculated for two different geometries with the dimensional parameters of 2.262 mm x 0.565 mm x 6 mm and 2.262 mm x 0.424 mm x 6 mm (length x width x thickness of substrate) and 40 μm wide silicon stiff film.

The eigenvalue buckling analysis gives a buckling profile which is conical and the wavelength is 82 μm. However, the non-linear post-buckling analysis shows a sinusoidal buckling profile with a wavelength decreasing with the decrement in the width of the stiff film from 61 μm to 54 μm as observed in the straight case. The load bearing capacity of this numerical model was found to

increase to 2% of strain. The out-of-plane displacement, stress distribution has been shown in Figure 34. A normalized plot for stresses in planar directions of the film is shown in Figure 35. The stress distribution shows a similarity with the straight case discussed in the previous section. The domination of the stresses in the direction of the silicon film and the decrement in the S22 near the long edges of silicon confirms the fact of the existence of the free traction boundary condition at the edges. Similar results of the displacement contours for a 100 μm wide silicon film case are showed in Figure 36.

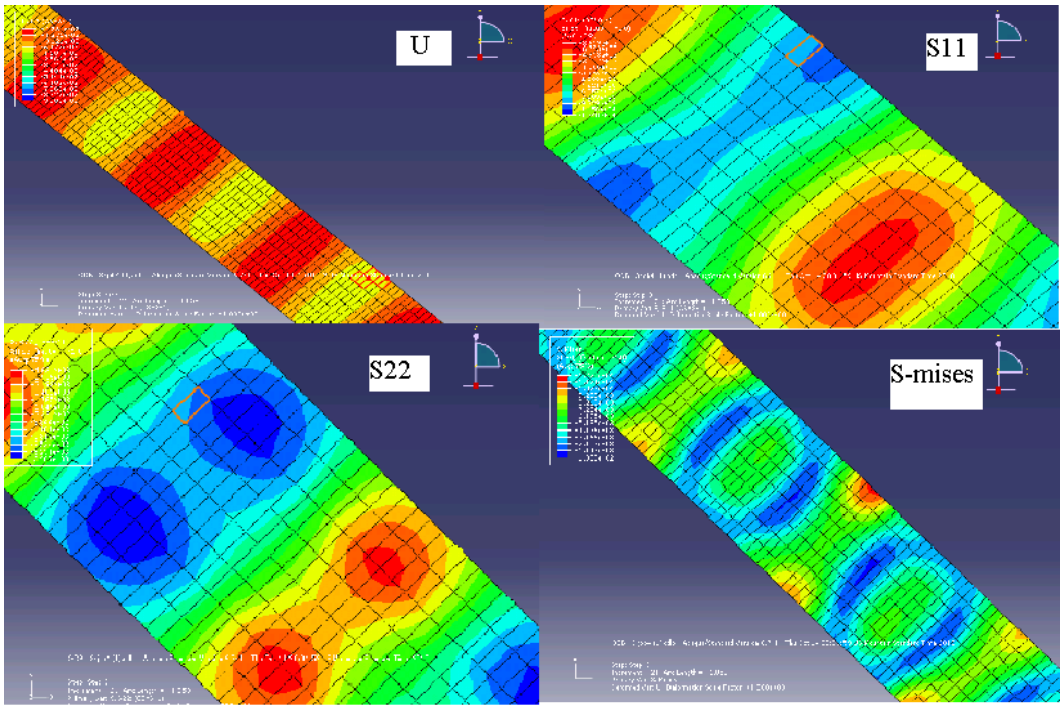

Figure 34 Post buckling result - 40 μm - Wavelength 54 μm

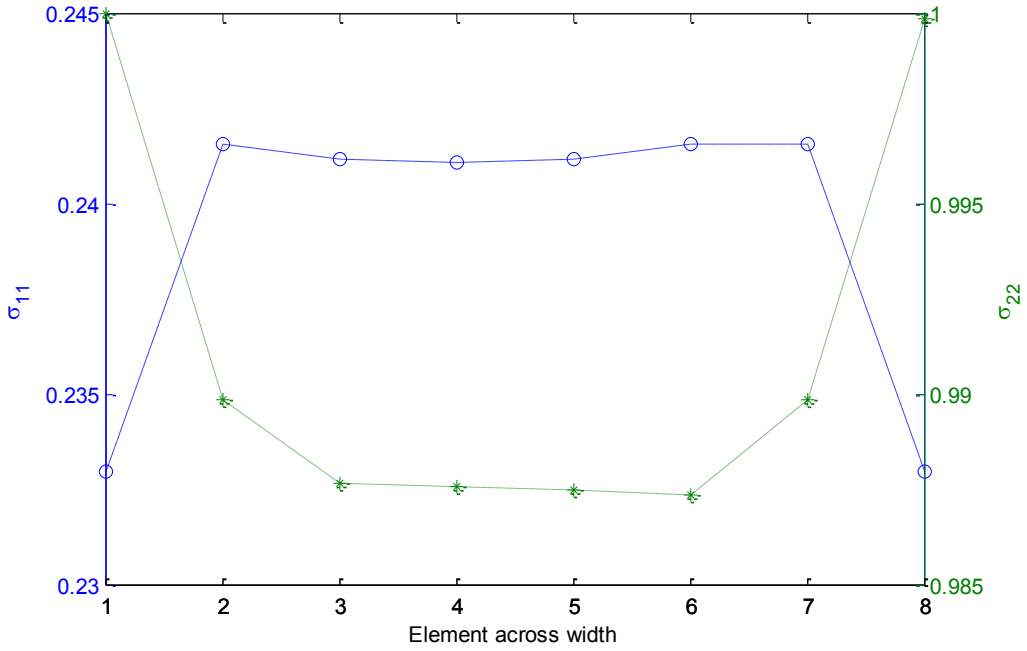

Figure 35 Stress plot for a 40 μm case

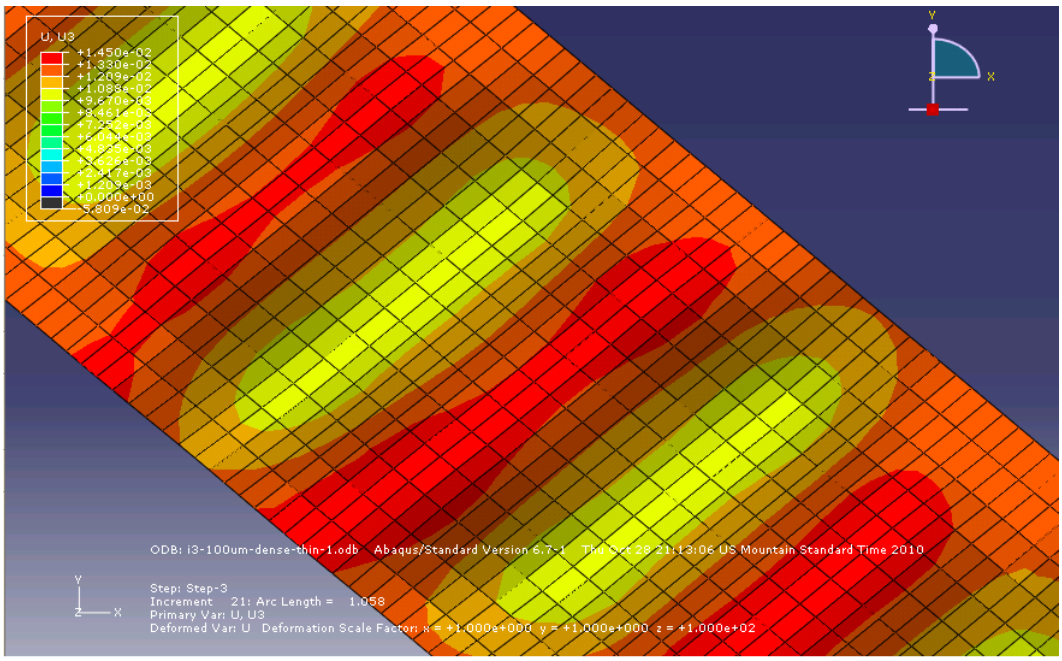

Figure 36 Out-of-plane displacement for 100 μm case

7 SUMMARY

The above study defines the relationship between the direction of pre-stress applied and the dimensional and material parameters of the model thus extending the study of the ordered buckling of stiff films on elastomeric substrates to an angled loading condition for different widths of the stiff film (ranging from 5 μm to 400 μm). It can concluded that the wavelength and the amplitude of the buckling profile have not changed with the direction of application of the pre-stress in case of narrow silicon films and are comparable to the case of application of the pre-stress in a direction parallel to the silicon film. Thus it can be concluded that the pre-stress direction does not affect the stress condition or the strains or buckling profile in the case of a narrow stiff film.

Future work includes the extension of the same procedure to wider silicon film in order to confirm the change in the direction of the buckling profile (>400 μm) from the direction perpendicular to the direction of the silicon film to the direction perpendicular to the direction of the application of pre-stress. The stress distributions in the angled case can be taken into consideration and an analytical solution can be formulated.

REFERENCES

Bowden, N, W T S Huck, K E Paul, and G M Whitesides. "The Controlled Formation of Ordered, Sinusoidal Structures by Plasma Oxidation of an Elastomeric Polymer ." *Applied Physics Letters*, 1999: 2557-2559 .

Bowden, N, Wilhelm T S Huck, Kateri E Paul, and George M Whitesides. "The Controlled Formation of Ordered, Sinusoidal Structures by Plasma Oxidation of an Elastomeric Polymer." *Applied Physics Letters* 75, no. 17 (1998): 2557-2559.

Chen, x, and J W Hutchison. "Herringbone Buckling Patterns of Compressed Thin Films on Compliant Substrates." *Journal of Applied Mechanics*, 2004: 597-603.

Choi, K M, and J A Rogers. "A Photocurable Poly(dimethylsiloxane) Chemistry Designed for Soft Lithographic Molding and Printing in the Nanometer Regime." *Journal of the American Chemical Society*, 2003: 4060-4061.

Choi, M K, J Song, D K Khang, H Jiang, Y Huang, and J A Rogers. "Biaxially Stretchable "Wavy" Silicon Nanomembranes." *Nano Letters*, 2007: 1655-1663.

Efimenko, K, M Rackaitis, E Manias, A Vaziri, L Mahadevan, and J Genzer. " Nested Self-similar Wrinkling Patterns in Skins." *Nature Materials* , 2005: 293-297.

Fu, Y Q, et al. " Evolution of Surface Morphology in TiNiCu Shape Memory Thin Films." *Applied Physics Letters*, 2006: 3.

Hanqing, Jiang, et al. "Finite Width Effect of Thin-Films Buckling on Compliant Substrate: Experimental and Theoretical Studies." *Journal of the Mechanics and Physics of Solids*, 2008: 2585-2598.

Hanqing, Jiang, Khang Dahl-Young, Song Jizhou, Sun Yugang, Huang Yonggang, and A Rogers John. "Finite Deformation Mechanics in Buckled Thin Films." *Proceedings of the National Academy of Sciences of the United States of America*, 2007: 15607–15612.

Harris, A K, P Wild, and D Stopak. "Silicone-Rubber Substrata - New Wrinkle in the Study of Cell Locomotion." *Science*, 1980: 177-179.

Harrison, C, C M Stafford, W H Zhang, and A Karim. " Sinusoidal phase grating created by a tunably buckled surface." *Applied Physics Letters* , 2004: 4016-4018.

Harrison, C, C M Stafford, W H Zhang, and A Karim. "Sinusoidal Phase Grating Created by a Tunably Buckled Surface." *Applied Physics*, 2004: 4016-4018.

Huang, R, and Z Suo. "Wrinkling of a Compressed Elastic Film on a Viscous Layer." *Journal of Applied Physics*, 2002b: 1135-1142.

Huang, R, H Yin, J Liang, J C Sturm, K D Hobart, and Z Suo. " Mechanics of relaxing SiGe islands on a viscous glass." *Acta Mechanica Sinica*, 2002: 441-456.
Huang, Z Y, W Hong, and Suo Z. "Evolution of Wrinkles in Hard Films on Soft Substrates." *PHYSICAL REVIEW E*, 2004: 70, 030601(R).

Huang, Z Y, W Hong, and Z Suo. "Nonlinear Analyses of Wrinkles in a Film Bonded to a Compliant Substrate." *Journal of Mechanics and Physics of Solids*, March 2005: 2101-2118.

Huck, W T S, N Bowden, P Onck, T Pardoen, J W Hutchinson, and G M Whitesides. "Ordering of Spontaneously Formed Buckles on Planar Surfaces." *Langmuir*, 2000: 3497-3501 .

Jiang, H, Y Sun, J.A Rogers, and Y Y Huang. "Mechanics of Precisely Controlled Thin Film Buckling on Elastomeric Substrate." *Applied Physics Letters* , 2007: 133119.

Jiang, H., Khang, D.-Y., Song, J., Sun, Y.G., Huang, Y., Rogers, J.A. "Finite Deformation Mechanics in Buckled Thin Films on Compliant Supports." *Proceedings of the National Academy of Sciences of the United States of America* , 2007: 15607-15612.

Jiang, X Y, et al. "Controlling Mammalian Cell Spreading and Cytoskeletal Arrangement with Conveniently Fabricated Continuous Wavy Features on Poly(dimethylsiloxane)." *Langmuir*, 2002: 3273-3280.

Kangmin, Niu, and Talreja Ramesh. "Modeling of Wrinkling in Sandwich Panels under Compression." *Journal of Engineering Mechanics*, August 1999: 875-883.
Khang, D Y, H Q Jiang, Y Huang, and J.A Rogers. "A Stretchable Form of Single-Crystal Silicon for High-Performance Electronics on Rubber Substrates." *Science*, 2006: 208-212.

Lacour, S P, J Jones, S Wagner, T Li, and Z G Suo. "Stretchable Interconnects for Elastic Electronic Surfaces." *Proceedings of the IEEE*, 2005: 1459-1467.

Lacour, S P, J Jones, Z Suo, and S Wagner. "Design and Performance of Thin Metal Film Interconnects for Skin-like Electronic Circuits." *IEEE Electron Device Letters*, 2004: 179-181.

Lacour, S P, S Wagner, R J, Li, T Narayan, and Z G Suo. "Stiff subcircuit islands of diamondlike carbon for stretchable electronics." *Journal of Applied Physics*, 2006: 6.

Lacour, S P, S Wagner, Z Y Huang, and Z Suo. "Stretchable Gold Conductors on Elastomeric Substrates." *Applied Physics Letters*, 2003: 2404-2406.

Ohzono, T, and M Shimomura. "Ordering of Microwrinkle Patterns by Compressive Strain." *Physical Review B*, 2004: 132202,1-4.

Schmid, H, et al. "Preparation of Metallic Films on Elastomeric Stamps and their Application for Contact Processing and Contact Printing." *Advanced Functional Materials*, 2003: 145-153.

Sharp, J S, and R A L Jones. "Micro-buckling as a Route Towards Surface Patterning." *Advanced Materials*, 2002: 799-802.

Stafford, C M, B D Vogt, C Harrison, D Julthongpiput, and R Huang. "Elastic Moduli of Ultrathin Amorphous Polymer ilms." *MacroMolecules*, 2006: 5095-5099.

Stafford, C M, et al. "A Buckling-based Metrology for Measuring the Elastic Moduli of Polymeric Thin Films ." *Nature Materials*, 2004: 545-550.

Stafford, C M, S Guo, C Harrison, and M Y M Chiang. "Combinatorial and High-throughput Measurements of the Modulus of Thin Polymer Films." *Review of Scientific Instruments*, 2005: 5.

Sun, Y, W M Choi, H Jiang, Y Y Huang, and J A Rogers. "Controlled Buckling of Semiconductor Nanoribbons for Stretchable Electronics." *Nature Nanotechnology*, 2006: 201-207.

Wagner, S, et al. "Electronic Skin: Architecture and Components." *Physica E-Low-Dimensional Systems & Nanostructures*, 2004: 326-334.

Wilder, E A, S Guo, S Lin-Gibson, M J Fasolka, and C M Stafford. "Measuring the Modulus of Soft Polymer Networks via a Buckling-based Metrology." *MacroMolecules*, 2006: 4138-4143.

Yoo, P J, K Y Suh, Park S Y, and Lee H H. "Physical self-assemblt of microstructures by anisotropic buckling." *Advanced Materials*, 2002: 1383-1387.